N.I.

RYAN

FACILITY FORM 602

N68-21998
(ACCESSION NUMBER)

(THRU)

60
(PAGES)

1
(CODE)

CR#94245
(NASA CR OR TMX OR AD NUMBER)

03
(CATEGORY)

FEASIBILITY STUDY
30 WATTS PER POUND
ROLLUP SOLAR ARRAY

Third Quarterly Report

Contract No. 951971

REPORT NO. 40067-3 15 APRIL 1968

N68-21998

This work was performed for the Jet Propulsion Laboratory, California Institute of Technology, as sponsored by the National Aeronautics and Space Administration under Contract NAS 7-100.

RYAN AERONAUTICAL COMPANY 5650 KEARNY MESA ROAD SAN DEIGO, CALIFORNIA

ABSTRACT

A quarter scale model of the solar array was fabricated during this reporting period. Demonstrations revealed two functional characteristics that could be improved. Preliminary design drawings are being revised and supporting analyses modified accordingly. A full scale demonstrations model is in process of construction, incorporating the design revisions being performed. A full scale wrap drum with representative wraps of the selected substrate materials and a simulated solar cell installation was subjected to vibration testing. Weight calculations have been revised to reflect the estimated effects of detail design changes. Performance of the solar array design is now projected as capable of producing 31.48 watts per pound of weight.

TABLE OF CONTENTS

SECTION	TITLE	PAGE
1.0	INTRODUCTION	1
2.0	TECHNICAL DISCUSSION	2
	2.1 DESIGN	2
	2.1.1 Mechanical/Structural	3
	2.1.1.1 Wrap Drum Support	3
	2.1.1.2 Wrap Tensioning System	4
	2.1.2 Electrical Design	5
	2.1.3 Materials and Processes	7
	2.1.3.1 Adhesive Systems	7
	2.1.3.2 Substrate Edge Attachment	8
	2.1.3.3 Plating Method for Aluminum Bus Bar	9
	2.2 TECHNICAL SUPPORT	11
	2.2.1 Drum Support and Guide Sleeve Mount Dynamic Analysis	11
	2.2.2 Drum End Plate Stress Analysis	18
	2.2.3 Substrate Attach Tab Stress Analysis	24
	2.2.4 Deployed Panel Dynamics	25
	2.2.5 Solar Cell Installation	34
	2.3 WEIGHT ANALYSIS	34
	2.4 TESTING-STOWED PANEL VIBRATION	45
3.0	FABRICATION-DEMONSTRATION MODEL	46
4.0	CONCLUSIONS	52
5.0	RECOMMENDATIONS	53
6.0	NEW TECHNOLOGY	54
7.0	REFERENCES	55

LIST OF ILLUSTRATIONS

FIGURE	TITLE	PAGE
1	Rollout Solar Array - Quarter Scale Model	2
2	Rollout Solar Array - Modified Drum Support and Tensioning Concept	6
3	Drum-Beam Guide Support	12
4	Cross Section of Drum End Plate	19
5	Power/Weight Monitor	44
6	Stowed Panel Vibration Test Setup	45
7	Wrap Drum Assembly	47
8	Deployable Beam - Forty-Five Foot Length, Deployed	48
9	Deployable Beam - Partially Unrolled	49
10	Deployable Beam With Corragated Rack Installation	50
11	Deployable Beam Showing Beam Splice Design	51

LIST OF TABLES

TABLE	TITLE	PAGE
1	RESULTS OF THERMAL VACUUM TESTS ON VARIOUS ADHESIVES	7
2	TENSILE SHEAR STRENGTH OF SILICONE RUBBER COATED CLOTH TO TITANIUM BONDS WITH RTV 3145	8
3	TENSILE SHEAR STRENGTH OF SILICONE RUBBER COATED CLOTH TO KAPTON BONDS WITH RTV 3145	9
4	PEEL STRENGTH OF PLATED ALUMINUM FOIL SOLDER CONNECTORS	10
5	DRUM SUPPORT AND GUIDE SLEEVE MOUNT ASSEMBLY	36
6	BEAM GUIDE SLEEVES	37
7	WRAP DRUM ASSEMBLY	38
8	SPACECRAFT MOUNT ASSEMBLY	39
9	PANEL ASSEMBLY	40
10	DEPLOYMENT/RETRACTION SYSTEM	41
11	WEIGHT SUMMARY	42

1.0 INTRODUCTION

This Third Quarterly Report is submitted by the Ryan Aeronautical Company to the Jet Propulsion Laboratory in accordance with Article I, Item (a) (2) (iv) and Article II, Item (a) (5) of Contract No. 951971. The report presents a summary of work accomplished from 1 January through 31 March 1968.

The discussion presented herein reports the collective efforts of Ryan and its associate contractor, Spectrolab Division of Textron Electronics, Inc. The data describes modifications to the drum support and drive system concepts and reports on progress made in the fabrication of a full scale demonstration model of the solar array.

2.0 TECHNICAL DISCUSSION

2.1 DESIGN

A quarter scale working model of the 250 square foot array was fabricated to substantiate the functional characteristics of the full size model (see Figure 1).

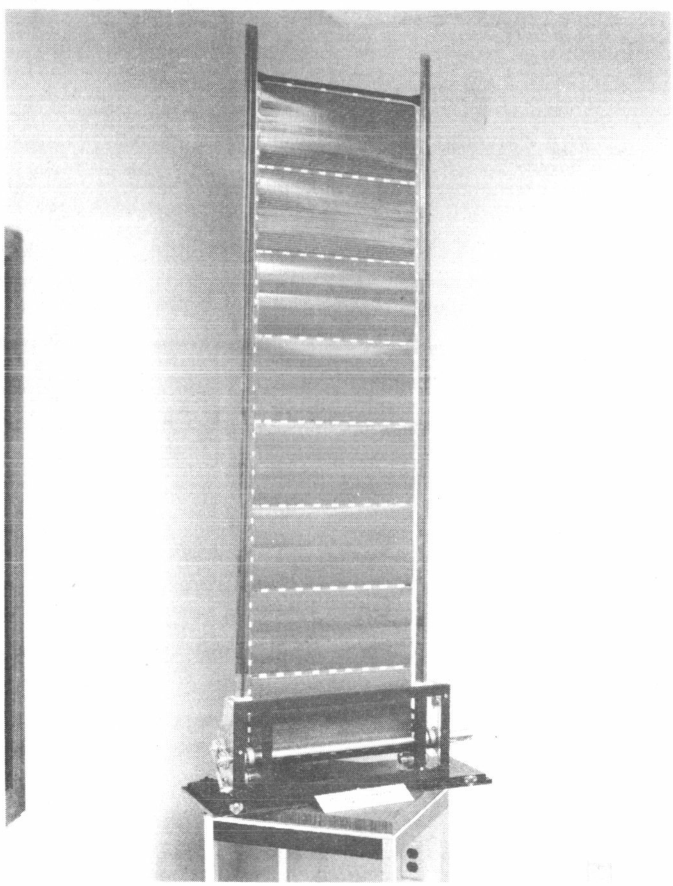

Figure 1 Rollout Solar Array - Quarter Scale Model

Demonstration and observation of the model proved the concept of the synchronized beam drive. Numerous deployments and retractions were made with no apparent tendency for either beam or substrate to move out of phase or to rack diagonally. It was evident that two features of the model could be improved by modification and the decision was made to incorporate these improvements into the design of the proposed flight-type model. The design changes will also be accomplished in the full scale demonstration model that is being fabricated.

2.1.1 Mechanical/Structural

The two features considered for change are: (1) the wrap drum support, (suspension and slide system) and (2) the wrap tensioning system.

2.1.1.1 Wrap Drum Support

In operation of the model it was apparent that an improved method was needed to maintain uniform drum contact with both the drive and idler rollers. The problem occurs because the movement of the drum center is restricted to a fixed line of travel by the spindle slide without opportunity to maintain the critical tangency point with the drive roller. The solution was to eliminate the idler roller and move the slide mechanism into a vertical position with its center passing through the drive roller.

The slide mechanism was altered to incorpoate four hardened steel rollers working in a hardened steel, channel-shaped track. As a result of moving the slide mechanism to the vertical position it was possible to reduce the size of the structure and simplify construction.

By eliminating the belt pulley on the end of the drive shaft, it was possible to simplify the limit switch mechanism and contain it in a more compact manner. The rotary limit switch is now located directly off the end of the drive shaft and is actuated through a pair of bevel gears instead of the cog belt as previously proposed.

2.1.1.2 Wrap Tensioning System

The wrap tensioning system, conceived to be simple in function, demonstrated certain deficiencies. One of the principal problems with the system was the expandable spring belt. On retraction it did not provide instant torque to the drum due to its expandable nature. This resulted in some initial slackness in the first wrap.

In the extension mode it was evident that the drive system needed some means of retarding the drum to prevent overrun of the wrapped beams. Their stored energy was working to relieve itself by uncoiling the beams.

These deficiencies prompted a decision to revert to the original tensioning system first proposed to JPL. This concept incorporated a separate tensioning and wrap motor, mounted directly to the drum spindle on the slide block. A description of the system follows.

The deployment and retraction motors work in unison, on both deployment and retraction cycles, through an electronic sensing system that controls power to each motor. This system is designed such that, when deployment is commanded, both deployment and retraction motor are energized. By adjustment of current input the deployment motor is the superior force and beam and substrate deployment takes place but a lagging action occurs with the retraction motor imposing a drag on the deployment motor. This has the effect of a braking action on the drum and prevents unwinding because of the stored energy in the beams.

In the retraction mode both motors are energized but the deployment motor in this case is controlled to lag the wrap motor, thus producing tension in the wraps. The electronic sensing system constantly monitors load and regulates current input to the motors. This system has both motors working concurrently, eliminating a need for a drag brake mechanism. The motors act as locks when current if off.

A redundant release clutch and a one way drive clutch is incorporated into the retraction motor mounting. Their function is to permit the array to operate with a failed retraction motor. Even though the retraction motor might fail to act as a brake, the array could be extended by the main deployment motors overriding the release clutch, causing it to slip. On retraction the deployment motors reverse and retract the unit; the one way drive clutch would overrun and allow the drum to turn. In this event, tight wraps would not necessarily be assured. The release clutch also serves as a safety measure to prevent damage to the beam drive strip corrugations should the drive and wrap motors ever be out of phase.

Redundancy in the drive system is maintained in the deployment mode by employing double motors working through a differential gearbox.

Figure 2 shows the modified array as discussed in Sections 2.1.1.1 and 2.1.1.2.

2.1.2 Electrical Design

The electrical design for the solar cell installation and its electrical circuitry has not changed from the concept previously reported. No further changes or modifications are contemplated in the Phase I effort.

The changes which have been made in the array deployment drive and tensioning system have resulted in relocating the power transfer slip rings (array-to-spacecraft). Previous reports have shown the electrical power rotary coupling at the same end of the drum as the drive motor installation. Power collection and lead-out will be relocated to the opposite end of the drum so that the new retraction motor installation and the existing drive motors are together at the same end of the wrap drum.

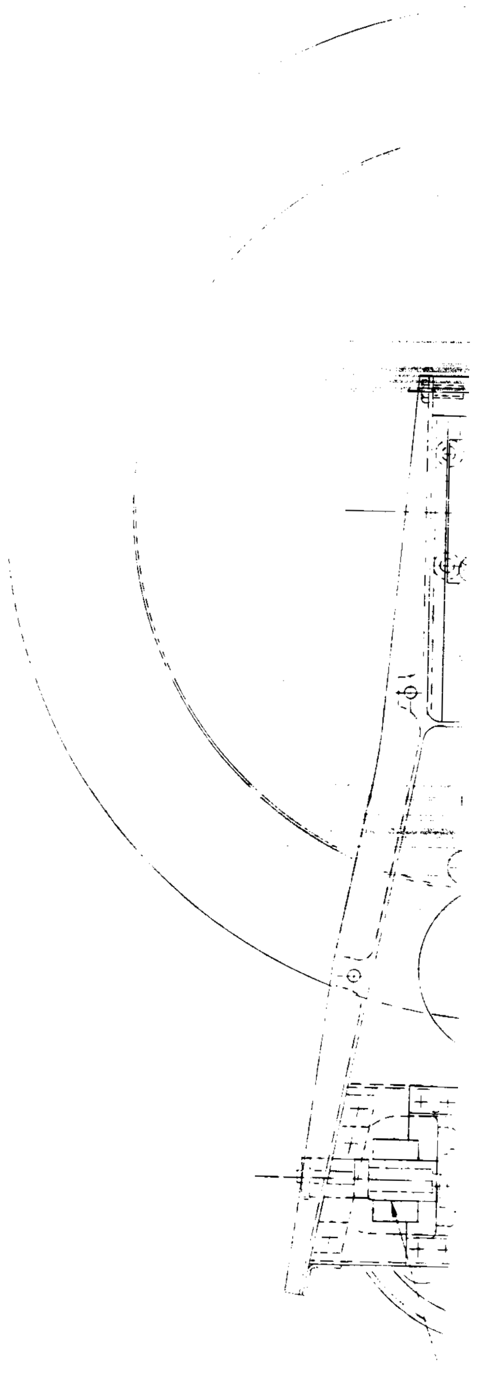

FOLDOUT FRAME 1

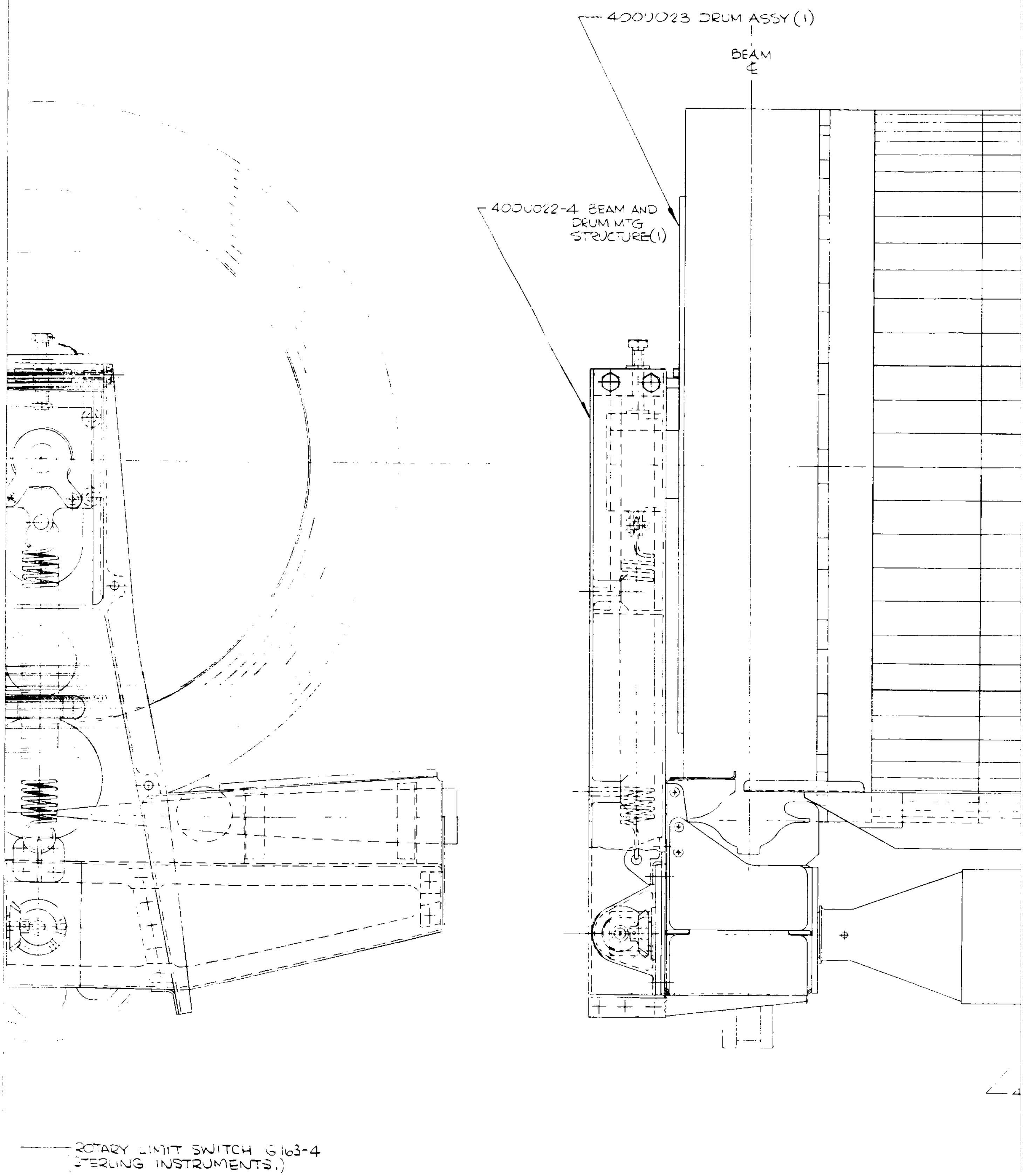

FOLDOUT FRAME 2

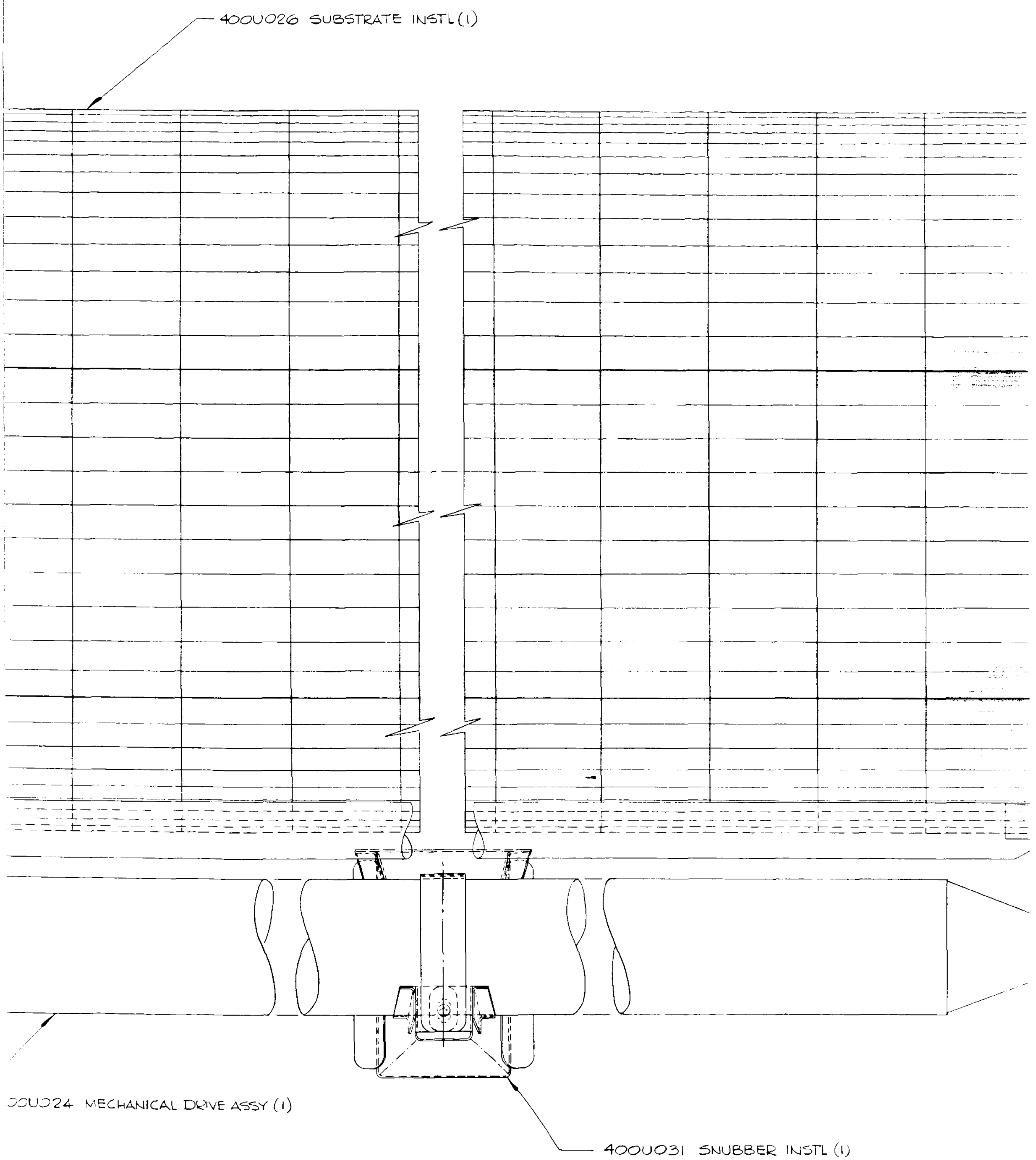

FOLDOUT FRAME 3

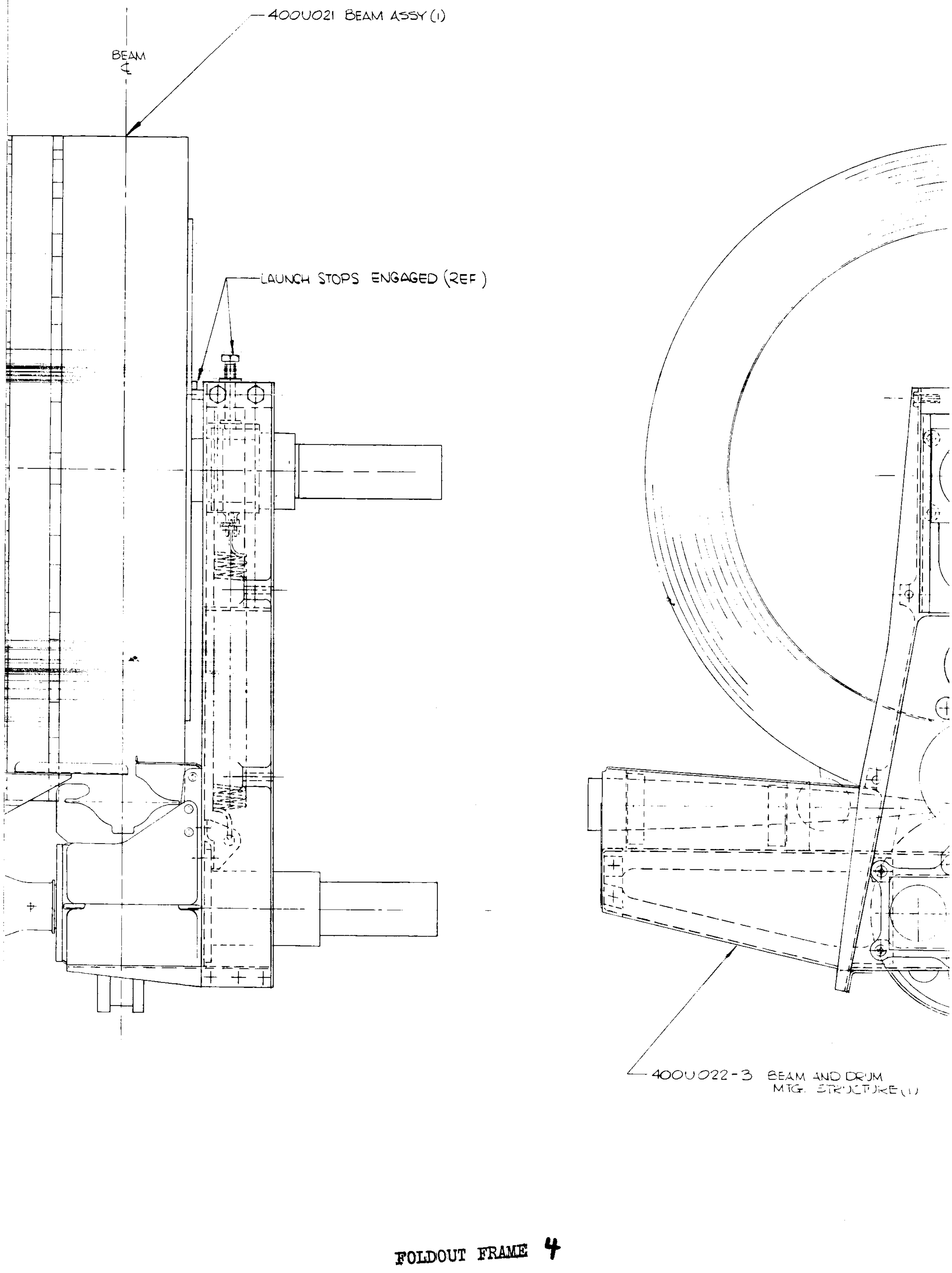

FOLDOUT FRAME 4

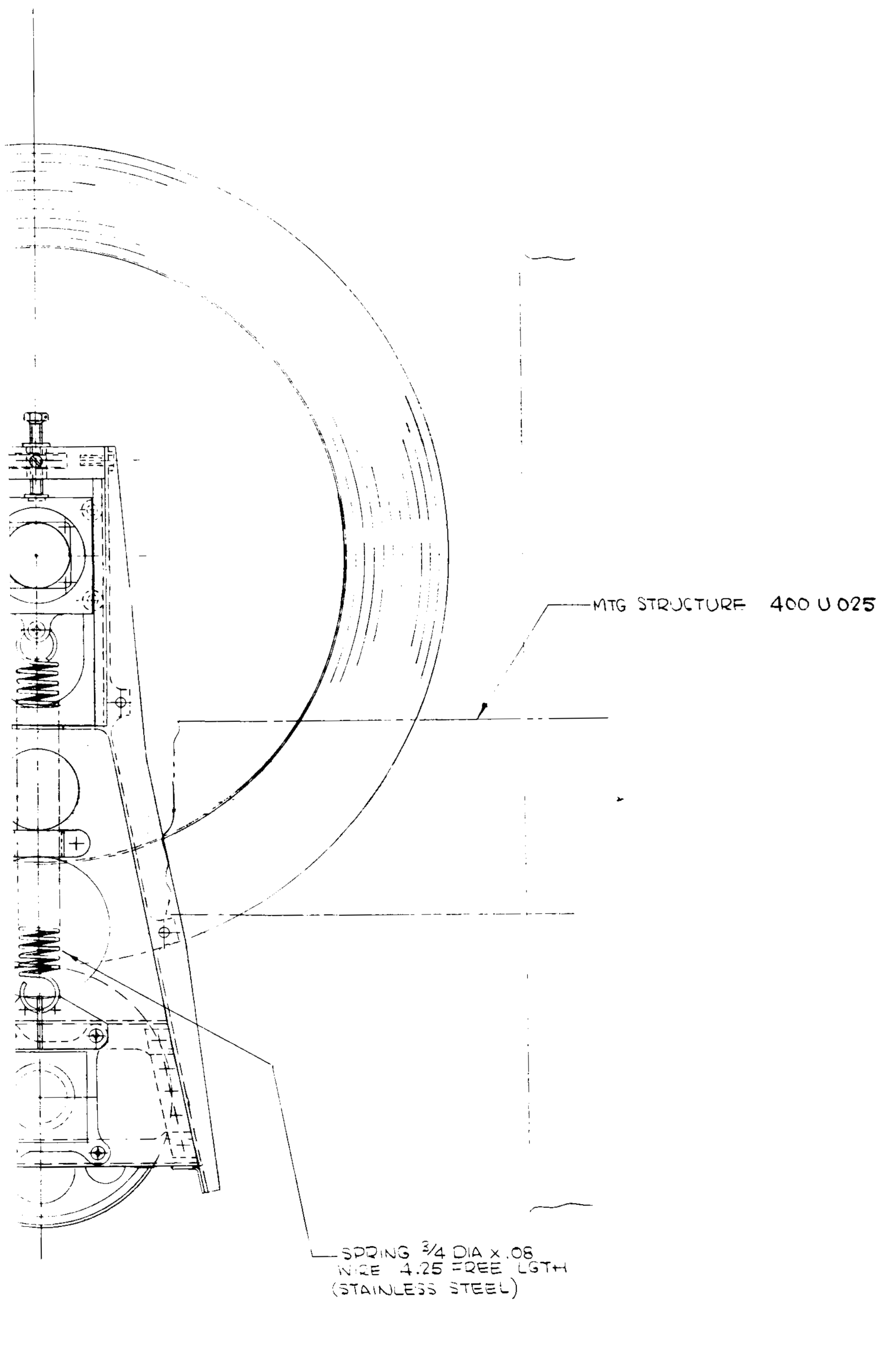

Figure 2 Rollout Solar Array - Modified Drum Support and Tensioning Concept

FOLDOUT FRAME 5

2.1.3 Materials and Processes

Additional testing was completed in this period to evaluate adhesive properties, substrate edge attachment strength and fabrication methods. A method of silver plating aluminum conductors to develop solderability, was investigated.

2.1.3.1 Adhesive Systems

Thermal vacuum tests on various adhesives were presented in the First Quarterly Report (Reference 1, page 154). Evaluation of RTV 3145 was conducted in this period using the same test method reported in the referenced document in order to include all candidate adhesives in the test group. Tensile specimens of RTV 3145 were subjected to ten cycles from -195°C to 140°C at 1×10^{7} Torr, with a 90 minute cycle and temperature stabilization dwell at the extreme temperatures. There was no decrease in tensile strength properties of the adhesives when compared to control samples. Test results are summarized in Table 1 which supplements the table presented in Reference 1, page 156.

TABLE 1

RESULTS OF THERMAL VACUUM TESTS ON VARIOUS ADHESIVES

Sample No.	Material	Before Test (grams)	After Test (grams)	Change (grams)	Tensile Strength (psi)
22 Control	RTV 3145	12.7795	12.7801	+0.0006	314*
23	RTV 3145	12.7155	12.7133	-0.0022	403
24	RTV 3145	12.8041	12.8014	-0.0027	402
25 Control	RTV 3145	-	-	-	414

*Air bubbles in specimen

2.1.3.2 Substrate Edge Attachment

Tests were conducted to measure joint strength and failure modes of the beam to substrate edge attachment. Tensile shear specimens of silicone rubber coated glass cloth, bonded to titanium and to Kapton, were prepared using RTV 3145 adhesive. Both Cohrlastic 1007 coated cloth and Cohrlastic 1005 coated one side cloth were evaluated. Specimens were 1.0 inch wide with 0.5 inch overlap. The tests indicate that a tensile shear strength of over 100 psi can be achieved with a failure mode characterized by separation of the silicone coating from the cloth fibers. The results of these tests are presented in Tables 2 and 3.

TABLE 2

TENSILE SHEAR STRENGTH OF SILICONE RUBBER COATED CLOTH TO TITANIUM BONDS WITH RTV 3145

Description	Primer	Shear Strength (psi) (average of 3 coupons)	Failure Mode
Cohrlastic 1007	None	128	Silicone coating to cloth
Cohrlastic 1007	1200 on Titanium	126	Silicone coating to cloth
Cohrlastic 1005 coated surface	1200 on Titanium	87	Silicone coating to cloth
Cohrlastic 1005 glass fiber surface	1200 on Titanium	115	RTV 3145 to cloth
Cohrlastic 1005 glass fiber surface	1200 on Titanium and glass fiber	138	Tensile failure of glass cloth at grip

TABLE 3

TENSILE SHEAR STRENGTH OF SILICONE RUBBER COATED CLOTH TO KAPTON BONDS WITH RTV 3145

Description	Primer	Shear Strength (psi) (average of 3 coupons	Failure Mode
Cohrlastic 1007	None	58	RTV 3145 to Kapton
Cohrlastic 1007	90 - 198 on Kapton	106	Silicone coating to cloth
Cohrlastic 1005 coated surface	90 - 198 on Kapton	75	Silicone coating to cloth
Cohrlastic 1005 fiber surface	90 - 198 on Kapton	94	RTV 3145 to cloth

It can be seen from the above results that the use of primer 90-198 (Dow-Corning) on the Kapton suface did not improve the bond strength between the RTV 3145 and the Kapton. It was also found that higher bond strengths are obtained if coated one side cloth is used and the bond is made to the un-coated side of the cloth.

2.1.3.3 Plating Method for Aluminum Bus Bar

The design of the array requires electrical connections to be made to the aluminum bus by soldering. A silver clad aluminum foil has been previously considered. However, it would be desirable to provide a silver plated surface, only in the areas to be soldered. The surface should be capable of soldering and desoldering so that rework can be performed if required.

Test samples consisting of a sheet of aluminum bonded between two sheets of Kapton were prepared with slots two inches long by 1/4-inch wide, provided in the Kapton. The aluminum connection areas, were brush-plated using Selectron No. 2 Activator, Selectron acid high speed copper and Selectron silver plating solution. Copper foil strips, 1/8-inch wide by 0.0015-inch thick were soldered to the plated surface using Kester 1544 flux and SN-63 solder. The strips were desoldered and soldered again, as noted, and pull tests performed as shown in Table 4.

TABLE 4

PEEL STRENGTH OF PLATED ALUMINUM FOIL SOLDER CONNECTIONS

Specimen	Plating Process	Solder/Desolder Cycles	Peel Strength (lbs/in. width)	Failure Mode
1	Activator/silver	1	4.5	Silver-aluminum separation
2	Activator/silver	1	4.9	Silver-aluminum separation
3	Activator/silver	5	2.1	Silver-aluminum separation
4	Activator/copper/silver	1	5.3	Copper-aluminum separation
5	Activator/copper/silver	1	6.8	Copper-aluminum separation
6	Activator/copper/silver	5	3.1	Aluminum tore
7	Activator/copper/silver	5	3.6	Copper-aluminum separation

The tests indicate either of the two plating systems provide acceptable adhesion. The Activator/copper/silver system is preferred.

2.2 TECHNICAL SUPPORT

Analysis performed during this reporting period is discussed in this section. Of primary concern during the period were (1) the effect of reposition of the wrap drum axis with respect to the mount bolt pattern, (2) deployed dynamic considerations and (3) determination of stowed panel dynamic characteristics by test.

2.2.1 Drum Support and Guide Sleeve Mount Dynamic Analysis

The redesign of the auxiliary drive system and the changing of position of the spacecraft mount attach bolts has altered the mounting dynamics. The drum and beam guide fitting, and dynamic idealization is shown in Figure 3. This section is concerned with the dynamic response of this support fitting with two sprung masses. The upper sprung mass is the drum and drum supported masses (point "F") and the second is the drive system and beam guide structure masses (point "A"). All stiffness assumptions are considered minimum for conservative purposes.

The weight of the sprung masses to be used are as follows, based on weights submitted in this report.

a. Deployment - Beam Guide

(1)	Deployment Retraction System*		4.878 pounds
(2)	Beam Guide Sleeves		1.191 pounds
(3)	Guide Sleeve Mount (15% of 1.564)		0.239 pounds
		TOTAL	6.308 pounds

Since during dynamic displacement both ends of the mounting system will be in phase, due to attachment through the drive shaft and the drum, 50% of the weight will be distributed to each end.

*The retraction drive system (1.004 pound) is included as part of the drum weight.

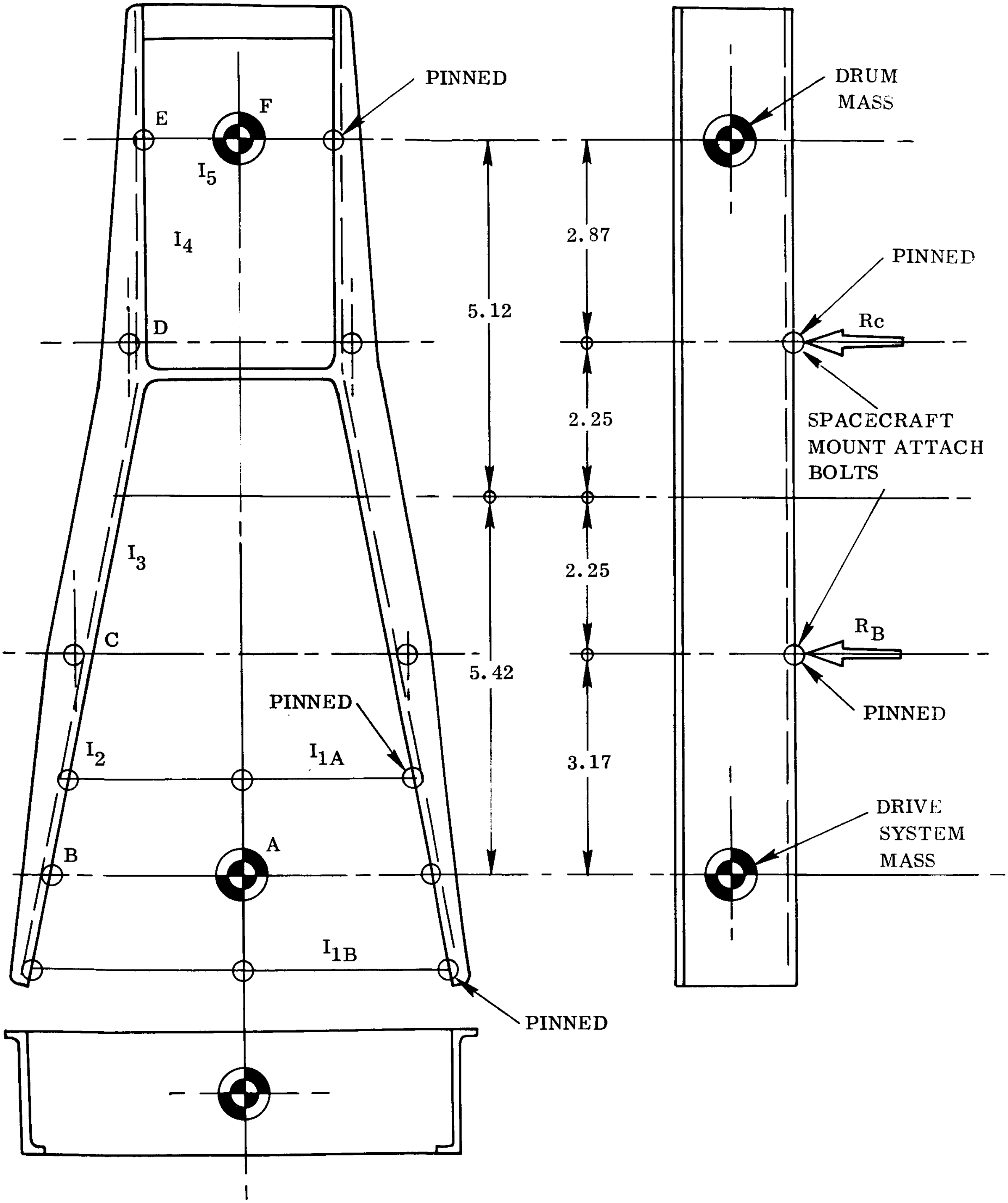

Figure 3 Drum-Beam Guide Support

$$W_s = 6.308/2 = 3.154 \text{ pounds/end} = W_1$$

b. Drum Assembly

(1)	Retraction Drive Motor	1.004 pound
(2)	Solar Cell Installation	44.627 pounds
(3)	Wrap Drum Assembly	9.400 pounds
(4)	Panel Assembly	8.731 pounds
(5)	Guide Sleeve Mount (50%, 1.564 pounds)	0.782 pound
	TOTAL	65.544 pounds

The weight will be distributed 50% to each end as above.

$$W_s = 64.544/2 = 32.272 \text{ pounds/side} - W_2$$

The dynamic response will be calculated by means of a 2 x 2 matrix assuming the masses concentrated as shown in Figure 3 and equally distributed to the side beams.

$$F_1 = -M_1 a_1 = + X_1 W_1 \left(\omega^2/g\right)$$

$$F_2 = -M_2 a_2 = + X_2 W_2 \left(\omega^2/g\right)$$

$$\left\{F\right\} = + \left(\omega^2/g\right) \left[\diagdown W \diagdown\right] \left\{X\right\} \qquad \text{(a)}$$

$$X_1 = K_{11} F_1 + K_{12} F_2 = \left(\omega^2/g\right) \left[K_{11} W_1 X_1 + K_{12} W_2 X_2\right]$$

$$X_2 = K_{21} F_1 + K_{22} F_2 = \left(\omega^2/g\right) \left[K_{21} W_1 X_1 + K_{22} W_2 X_2\right]$$

$$\left\{X\right\} = \left[K_{ij}\right] \left\{F\right\} = \left(\omega^2/g\right) \left[K_{ij}\right] \left[\diagdown W \diagdown\right] \left\{X\right\} \qquad \text{(b)}$$

K_{ij} = influence coefficient for deflection at point "i" due to load at point "j".

$I_{1A} = I_{1B}$, since the motor mounting case is very stiff (1)

$P_1 = P_2 = P_A/2$

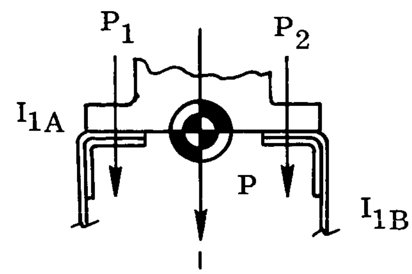

$\Delta_1 = WL_1^3/48EI$

$L_1 = 5.0$ inches, $L_2 = 6.0$ inches

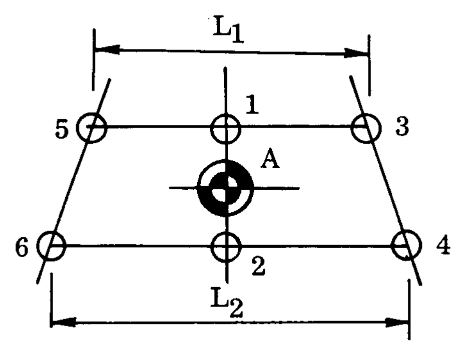

$I_x = (2)\ (.50 - .04)\ (.04)\ (.40 - .02)^2 + (.04)\ (.8)^3/12$

$I_x = .007034$

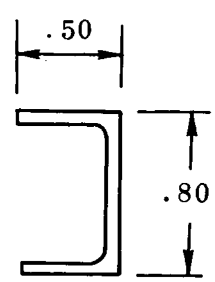

$$\Delta_1 = (P_A/2)L_1^3/48EI$$

$$\Delta_1 = P(5.0)^3/96\ (6.5)\ (10^6)\ (.007034) = 125\ P_A/4.3892\ (10^6)$$

$$\Delta_2 = (6.0)^2\ P_A/4.3892\ (10^6) = 216\ P/4.3892\ (10)^6$$

$$\Delta'_{A1} = (\Delta_1 + \Delta_2)/2 = (125 + 216)\ P/2\ (4.3892)$$
$$10^6 = 3.885\ P_A/10^6$$

This is for both ends.

$$\Delta_{A1} = (2)\ (3.885)\ P/10^6 = 7.770\ P_A/10^6 \text{ for one end.}$$

$$I_5 = b_{eq}h^3/12 = .24\ (1.00)^3/12 = .0200 \qquad (2)$$

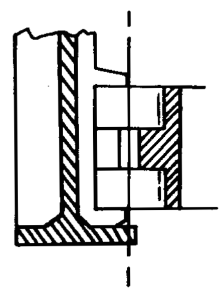

L_5 = 4.00 inches, assumed simply supported.

$$\Delta F_3 = P_F L_F^3/48EI$$

$$\Delta F_3 = P_F\ (4.0)^3/48\ (6.5)\ (10^6)\ (.02) = 10.256\ P_F/10^6$$

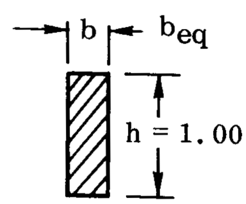

$$I_3 = (1.75)^3\ (.08)/12 + 2\ (.08)\ (.56)\ \left[(1.75 - .08)/2\right]^2 \qquad (3)$$

$$I_3 = .0982$$

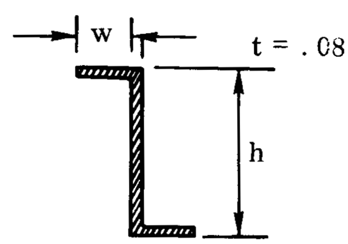

$$I_2 = .035729 + .111556\ (.5) - .091507 \qquad (2)$$

$$I_4 = .035729 + .111556\ (.45) = .085479 \qquad (3)$$

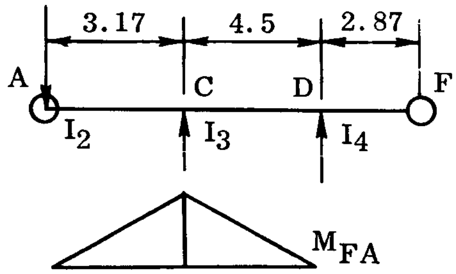

For a load at point "A",

$$\Delta_{A2} = \Delta_{cant} + L_A\ \theta_C$$

$$\Delta_{A2} = (P/2)L_A^3/3EI_2 + (L_A)\ M_O L_{CD}/3EI_3$$

$$M_O = (P_A L_A/2)$$

$$\Delta_{A2} = (PL_A^{\ 2}/6E)(L_A/I_2 + L_{CD}/I_3)$$

$$= \left[P\ (3.17)^2/6\ (6.5)\ 10^6\right] \left[3.17/.091507 + 4.5/.0982\right]$$

$$= 20.733\ P/10^6$$

$$\Delta F1 = L_4\theta_D = L_4 M_O L_{CD}/6EI_3 = PL_A L_4 L_{CD}/12EI_3$$

$$\Delta F1 = P(3.17)\ (4.5)\ (2.87)/12\ (6.5)10^6\ (.0982) = 5.345\ P/10^6\ \text{(Pos.)}$$

$$\Delta = KF \simeq KP \qquad K = \Delta/P$$

$$\Delta_A = \Delta_{A1} + \Delta_{A2} = (7.770 + 20.773)P/10^6 \qquad \text{(Pos.)}$$

$$K_{11} = \Delta_A/P = 28.503/10^6$$

$$K_{21} = \Delta_{F1}/P = 5.345/10^6 = K_{12}$$

For a load at point "F",

$$\Delta_{F2} = \Delta_{cant} + L_F\theta_D = PL_F^{\,3}/6EI_4 + PL_F^{\,2}\, L_{DC}/6EI_3$$

$$\Delta_{F2} = \left[P\ (2.87)^2/39\ (10^6)\right]\ \left[2.87/.085479 + 4.5/.0982\right]$$
$$= 16.769\ P/10^6$$

$$\Delta_{A3} = L_A\theta_C = L_A\ (PL_FL_{CD}/6EI_3) = \Delta_{F3}$$

$$\Delta_F = \Delta_{F2} + \Delta_{F3} = (16.769 + 10.256)\ P_F/10^6$$
$$= 27.025\ P_F/10^6 \quad \text{(Pos.)}$$

$$K_{22} = \Delta_F/P_F = 27.025/10^6$$

Substituting in matrix,

$$\begin{Bmatrix} X_1 \\ X_2 \end{Bmatrix} = (\omega^2/g10^6) \begin{bmatrix} 28.503\ (3.154) & 5.345\ (32.272) \\ 5.345\ (3.154) & 27.025\ (32.272) \end{bmatrix} \begin{Bmatrix} X_1 \\ X_2 \end{Bmatrix}$$

Point "1" Point "A" and Point "2" ≈ Point "F" g = 386.1

$$\begin{Bmatrix} X_1 \\ X_2 \end{Bmatrix} = (\omega^2/g10^6) \begin{bmatrix} 89.898 & 172.494 \\ 16.858 & 872.151 \end{bmatrix} \begin{Bmatrix} X_1 \\ X_2 \end{Bmatrix}$$

Solving the fundamental mode shape by reiteration, the normalizing factor and normalized mode shape is found to be,

$$\begin{Bmatrix} X_1 \\ X_2 \end{Bmatrix} = 875.850 \begin{Bmatrix} .2194 \\ 1.0000 \end{Bmatrix}$$

$$\omega^2/g(10^6) = 1/875.85$$

$$f_n = \omega/2\pi = (1/2\ \pi)\ \sqrt{386.1\ (10^6)/875.85} = \underline{\underline{105.7}}\ \text{cps}$$

Before the design was changed, the above frequency was 79.6 cps, (see Reference 1). The effect of the increased frequency resulting from the design change serves to reduce the dynamic deflection of the drive system mass. However, since this frequency also indicates motion of the wrap drum mass, which was previously fixed at the center of the mount bolt pattern, consideration will be given to effect on loads in the wrap drum spindle, drum end plates and the spacecraft mounts. This data will be presented in the final report.

2.2.2 Drum End Plate Stress Analysis

The drum end plate consists of the honeycomb end plate and an attach hub for mounting the end bearings (see Figure 4). Since the degree of fixity to the drum is dependent on redundant supporting structure, conservative assumptions are made for stress calculation purposes. Loads used for analysis are taken from the Second Quarterly Report, Section 2.2.3.2, pages 37-40.

Consideration is not given in this report to effects of possible increased loading with the wrap drum, now located eccentrically with respect to the spacecraft mount bolt pattern. This effect will be discussed in the final report.

Hub Analysis

$$P_N = P_{AX}/n + M_O/n_2 h$$

$$n = 6 \text{ bolts}$$

$$n_2 = 2 \text{ bolts}$$

$$h = D_B \cos 30° = 2.4\ (.86603)$$

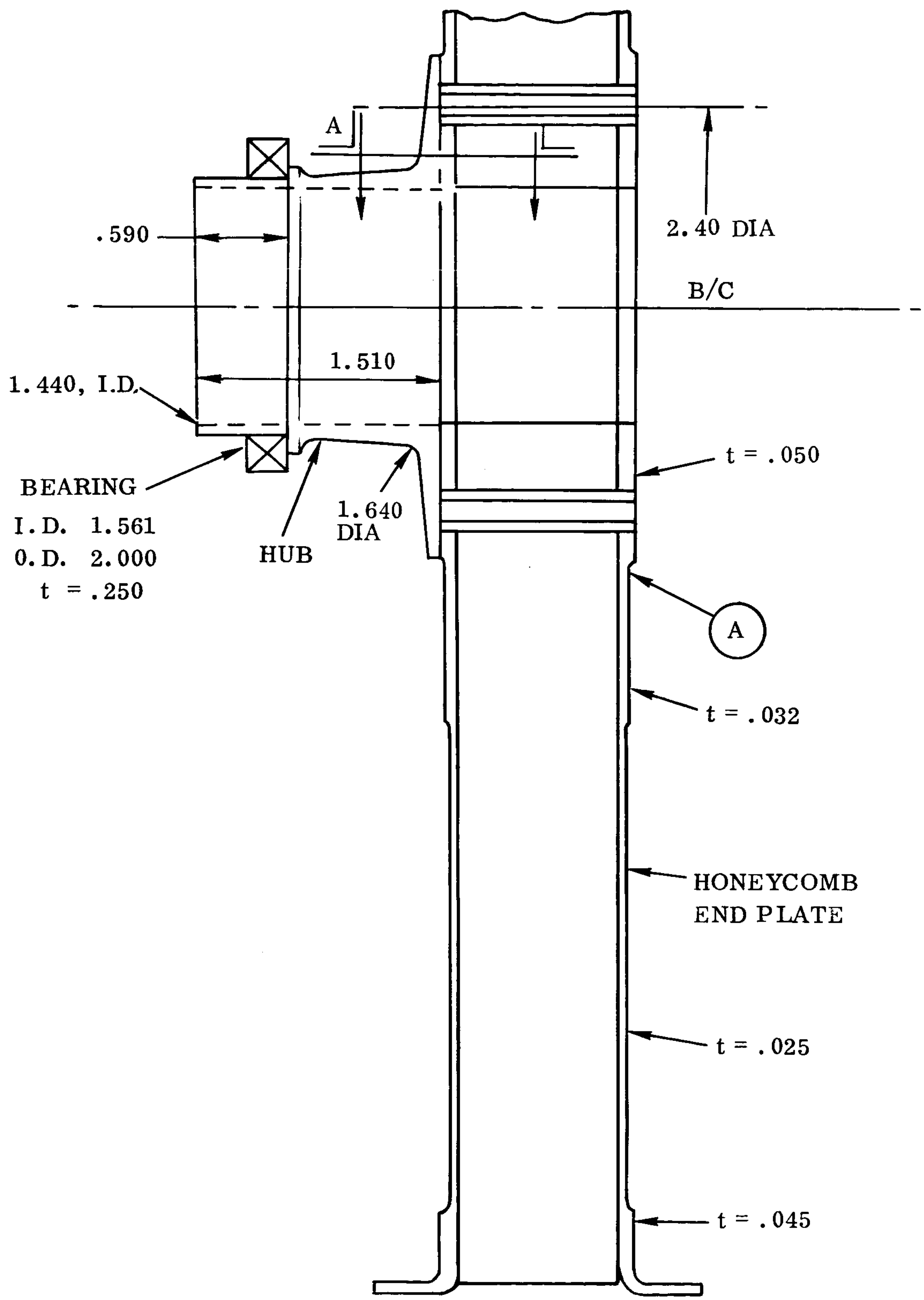

Figure 4 Cross Section of Drum End Plate

$h = 2.078$

$P_{AX} = 814.99$ lb., limit

$P_R = 715.68$ lb., limit

$M_O = d_2 P_R = 1.05\ P_R$

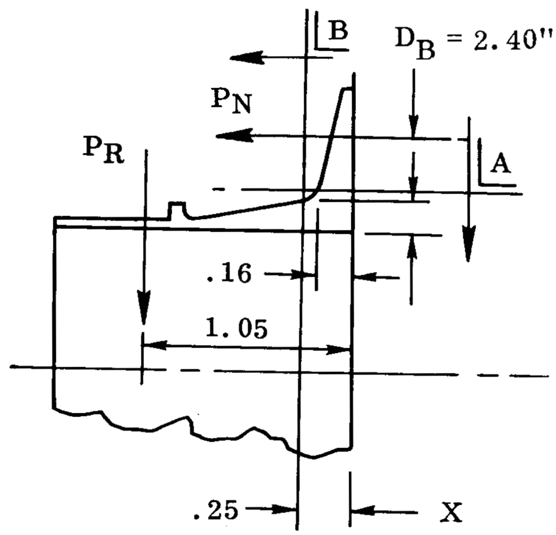

$P_N = 814.99/6 + 105\ (715.68)/2\ (2.078)$

$P_N = 316.66$ lb./bolt

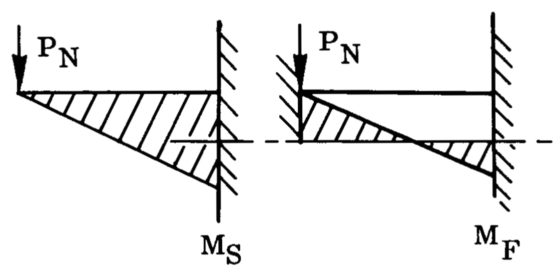

Section "A-A", $d_3 = .28$

$f_b = 6M/bt^2 = 6\ Kd_3\ P_N/bt^2$

$M_S = K_S d_3 P_N \qquad K_S = 1.00$

$M_F = K_F d_3 P_N \qquad K_F = .5$

Use K = .80, equal to 40% edge fixity at P_N.

f_b = (6) (.80) (.28) (316.66)/(.9) $(.16)^2$ = 18,472 psi, limit

F_{ty} = 20,000 psi; AZ31B - H24 magnesium

Shear,

f_s = KP_N/A_S = KP_N/bt = 1.5 (316.66)/.9(.16) = 3,299 psi, limit

F_{su} = 15 Ksi F_{sy} = 16 (20 Ksi/34) = 9,400 psi

M.S. = F_{ty}/f_{by} =1 = 20/18.472 -1 = $\underline{\underline{+.08}}$ limit

End Plate Analysis

The plate is considered as a fixed hub, partially fixed (20%) at the outer edge. Maximum stress occurs at the inner edge, the hub attach area (r = b), and is calculated as follows:

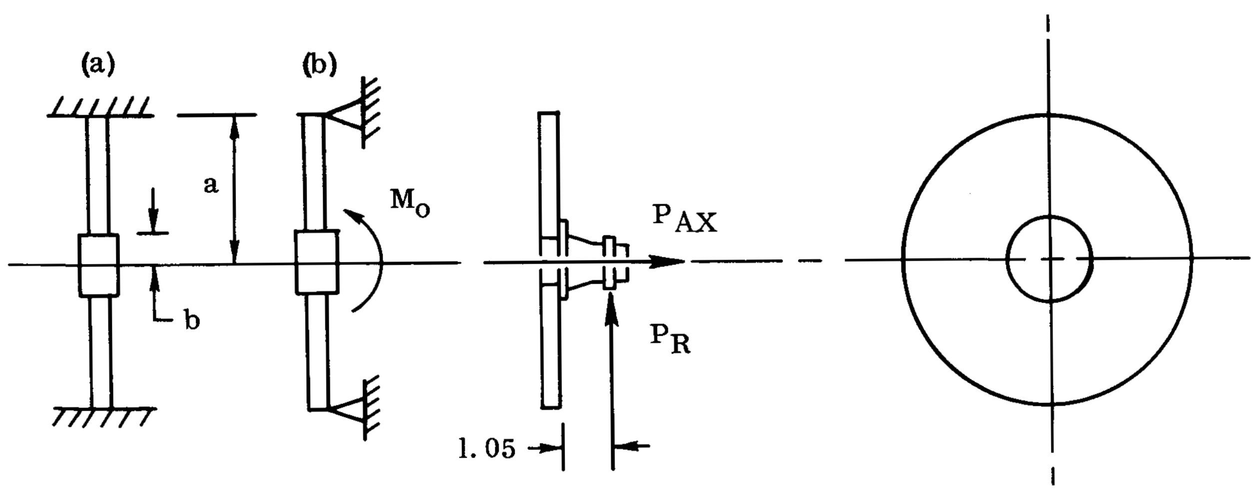

Reference 3, pages 42, 61.

Dimension "b" is assumed to be 1.5 inches since there is a 3.0 inch diameter reinforcing pad on the honeycomb face sheet.

a/b = 6.0/1.5 = 4.0

(1) For axially loaded plate,

(a) $f_b = K_F P/h^2 = 6\ M_{EQ}/h^2,\ K_F = .933$ (Case 6 of Ref. 3)

(b) $f_b = K_{SS} P/h^2 = 6\ M_{EQ}/h^2,\ K_{SS} = 1.514$ (Case 8 of Ref. 3)

For 20% outer edge fixity,

$$K = K_{SS} - .20\ (K_{SS} = K_F) = 1.514 - .20\ (1.514 - .933) = 1.398$$

$$f_b = KP/h^2 = 6\ M_{EQ}/h^2$$

$$M_{EQ} = KP/6 = 1.398\ P/6 = .233\ P_{AX}$$

For honeycomb, $I = 2\ Ad^2 = 2t_F d^2$

$$c/I = \left[(t_c + 2t_f)2\right] \Big/ \left[2t_f\ (t_f + t_c)^2/4\right]$$

$$c/I = (t_c + 2t_f)/t_f\ (t_f + t_c)^2$$

For $t_c = 1.00,\ t_f = .032$ $\quad P_{AX} = 815$ lb., limit

$$c/I = 1.064/(.032)\ (1.032)^2 = 31.22$$

$$f_{b1} = M_{EQ} c/I = (.233\ P_{AX})\ (31.22)$$

$f_{b1} = \pm\ \underline{\underline{5,929}}$ psi, limit at radius "b", radially.

(2) For moment loaded plate,

$M_o = P_R d = 715.7\ (1.05)$ inch lb., limit

(Reference 4, pages 194 and 216 for full thickness plate, Cases 5 and 10.)

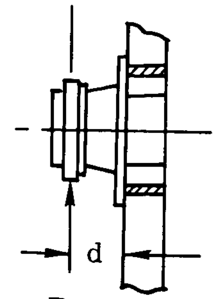

$f_{b2} = \beta M/ah^2 = 6\ M_{EQ}/h^2$

$M_{EQ} = \beta M/6a$

$b/a = 1.5/6.0 = .25 \quad \beta = 5.00$, est.

$M_{EQ} = \beta M/6a = (5.0)\ (715.7)\ (1.05)/6\ (6.0)$

$M_{EQ} = 104.41$ inch lb., limit

Then, for honeycomb

$f_{b2} = M_{EQ}\ (c/I) = (104.4)\ (31.22) = \pm \underline{\underline{3,259}}$ psi, limit

$f_b = f_{b1} + f_{b2} = 5929 + 3259 = \pm \underline{\underline{9,188}}$ psi, limit at radius "b" at juncture of 3.0 diameter - .050 reinforcing ring.

For 7075 aluminum face plate,

$M.S. = F_{ty}/f_b - 1 \qquad \rightarrow \underline{\underline{\text{High}}}$

Stress at outer edge is calculated as follows, assuming an outer edge fixity of 80%,

$$f_{b1} = (.80)\ (3\ P_{AX}/2\pi h^2)\ \left[1 - 2b^2\ (\ell n\, a/b)/(a^2 - b^2)\right]$$

$$f_b = 6M/h^2 \qquad M_{EQ} = f_b h^2/6$$

$$M_{EQ} = (.80)\ (P_{AX}/4\pi)\ \left[1 - 2b^2\ (\ell n\ a/b)/(a^2 - b^2)\right]$$

$$a/b = 6.0/1.5 = 4.0,\ \ell n_c\ 4.0 = 1.38629$$

$$M_{EQ} = (.20\ P_{AX}/\pi)\ \left[1 - 2\ (1.5)^2\ (1.38629)/6.0^2 - 1.5^2)\right]$$

$$M_{EQ} = .20\ P_{AX}\ (1.185)/\pi = .0754\ P_{AX}$$

$$c/I = (t_c + 2t_f)/t_f\ (t_f + t_c)^2 = 1.05/(.025)\ (1.025)^2$$

$$c/I = 39.98$$

$$f_{b1} = M_{EQ}\ (c/I) = .0754\ (815)\ (39.98)$$

$b_{b1} = \underline{\pm\ 2,457}$ psi, limit. This is low for hub bending; assume a ratio of distribution in proportion to the axial bending stress.

$$f_{b2} = f'_{b2}\ (f_{b1}/f'_{b1}) = 3259\ (2457/5929) = 1,351$$

$f_b = f_{b1} + f_{b2} = 2457 + 1351 = \underline{\underline{\pm\ 3,808}}$ psi, limit

2.2.3 Substrate Attach Tab Stress Analysis

The following analysis is conducted for possible loads transferred to the flattened beams, through the attach tabs. This can occur during drum axial vibration of the stowed panel; see the Second Quarterly Report, Section 2.2.5.1.

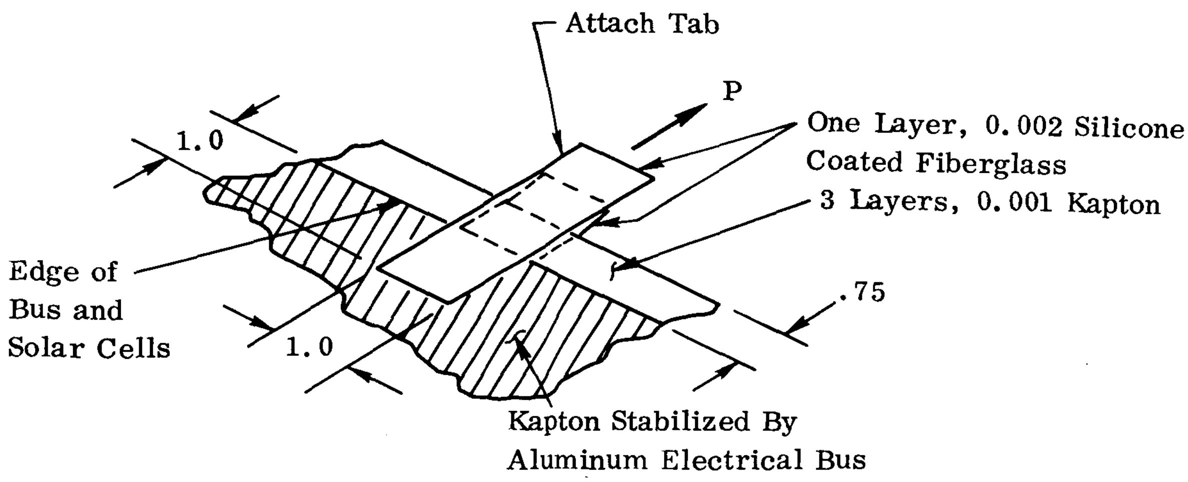

$P = 10$ lbs., limit

$P_{allow.} = 70$ lbs.,/in., in warp direction for the fiberglass tab, Reference 5.

$$f_s \begin{pmatrix}\text{adhesive in}\\ \text{bus area}\end{pmatrix} = \frac{P}{\text{area}} = \frac{10}{1 \times 1} = \underline{\underline{10}} \text{ psi}$$

$$f_s \begin{pmatrix}\text{adhesive at}\\ \text{beam attach}\end{pmatrix} \quad \frac{P}{\text{area}} = \frac{10}{1 \times .5} = \underline{\underline{20}} \text{ psi}$$

F_s = 138 psi, Ryan test data (see Section 2.1.3.2, Table 2)

M.S. = $\rightarrow$ <u>High</u>

This condition will exist, assuming that such restraint provisions are necessary for the axial vibration consideration. Analysis also indicates that a similar load magnitude will develop with respect to the panel under an end-on solar flux condition. The need for such restraint provisions cannot be resolved until an axial vibration test is conducted on the stowed panel. This will determine if sufficient axially-directed friction exists between adjacent panel wraps on the drum (array in stowed condition) to limit relative displacement of panel wrap(s) during vibration.

2.2.4 Deployed Panel Dynamics

Cantilevered Panel Mode

This analysis reflects the stiffness values of the beams which were made for the full scale demonstration model. These parts developed a full depth of 1.5 inches rather than 1.7 inches shown on the engineering drawing.

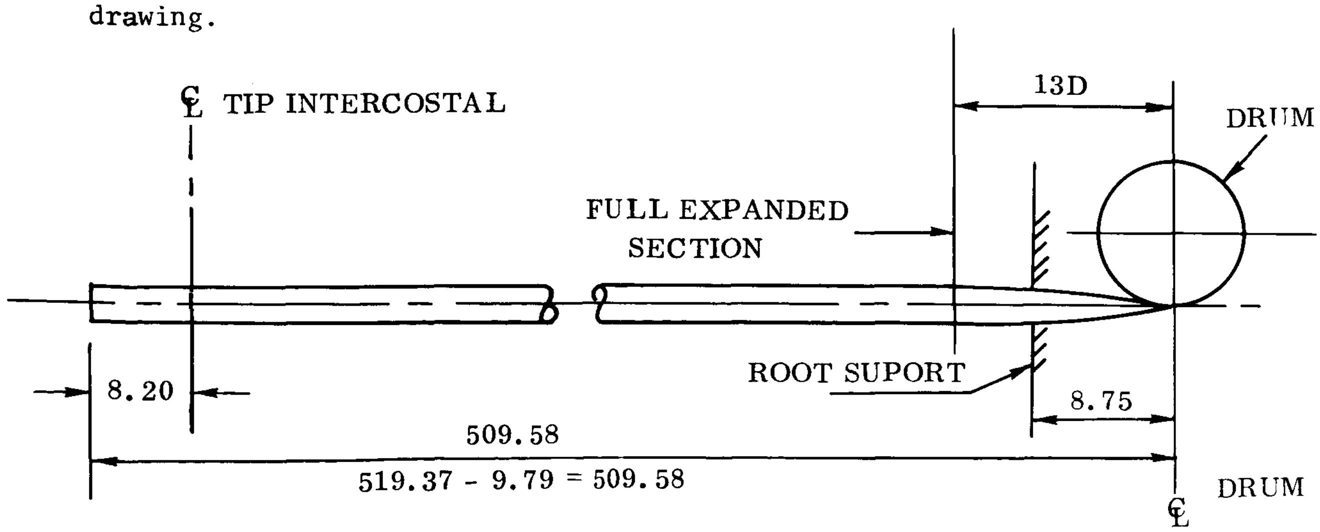

Distributed weight on beam,

Solar Cell Installation	44.50 lb.
Substrate and Beams	8.46 lb.
Tip Intercostal	0.28 lb.
TOTAL	53.24 lb.

The above weight is assumed distributed over the length of the two beams, starting at the root support. The effective beam length for dynamic consideration is therefore considered to be 512.0 inches.

$$w = 53.24/(2)\ (49. \quad .053778 \text{ lb./in./beam}$$

$$d = 509.58 - 8.75 - 8.20 = 492.63\text{; use 495 inches.}$$

The cross-section at the right has been scaled from a sample beam and modified slightly to conform to the detail drawing of the beam.

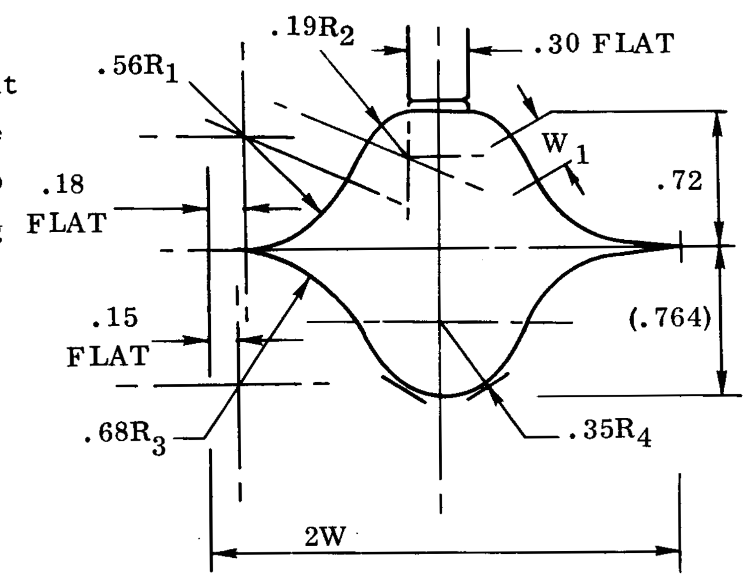

For top half beam,

$$L = 3.00/2 = 1.5$$

$$L = .18 + .15 + (R_1 + R_2)\ \alpha + w_1 = 1.5$$

$$h = .72 = (R_1 + R_2)\ (1 - \cos\alpha) + w_1 \sin\alpha$$

$$1.5 - .18 - .15 = (R_1 + R_2)\ \alpha + w_1 = (R_1 + R_2)(\alpha^\circ\pi/180) + w_1$$

$$= (R_1 + R_2)\ (\alpha\pi/180) + w_1 = 1.17 \qquad (1)$$

$$(R_1 + R_2)\ (1 - \cos\alpha) + w_1 \sin\alpha = .72 \qquad (2)$$

$$(R_1 + R_2) = .56 + .19 = .75$$

$$\alpha_1\ (.75)\ (\pi/180) + w_1 = 1.17$$

$$\left[.01309\ (\alpha) + w_1 = 1.17\right| \quad -$$

$$(.75)\ (1 - \cos\alpha)/\sin\alpha + w_1 = .72/\sin\alpha \qquad (2)$$

$$- .01309\ \alpha + (.75)\ (1 - \cos\alpha)/\sin\alpha = .72/\sin\alpha - 1.17$$

$$(.75)\ (1 - \cos\alpha) + \sin\alpha\ (1.17 - .01309\ \alpha) = .72$$

Solving the preceding equation by trial and error,

$$\alpha_1 = 64^\circ\ 03' = 64.05^\circ$$

$$w_1 = 1.17 - .01309\ (64.05) = .33159$$

$$W = .18 + (R_1 + R_2)\sin\alpha + w\cos\alpha$$

$$W = .18 + .75\ (.89918) + .33159\ (.43759) + .15 = 1.1495$$

For lower half,

$$R_3 + R_4 = .68 + .35 = 1.03$$

$$W = 1.1495 = .15 + w_2 \cos\alpha + (R_3 + R_4)\sin\alpha \qquad (3)$$

$$w_2 \cos\alpha + 1.03 \sin\alpha = .9995$$

$$L = 1.5 = .15 + (R_3 + R_4)\ \alpha + w_2$$

$$w_2 = 1.35 - 1.03\ (\alpha\pi/180)$$

$$w_2 = 1.35 - .01798\ \alpha^\circ \qquad \text{Substitute in (3)}$$

$$(1.35 - .01798\ \alpha^\circ)\cos\alpha + 1.03 \sin\alpha = .9995$$

Solving by reiteration,

$$\alpha = 69^\circ\ 48' = 69.8^\circ$$

$$w_2 = 1.35 - 01798\ (69.8) = .0950$$

$$h_2 = (R_3 + R_4)\ (1 - \cos\alpha) + w_2 \sin\alpha$$

$$= 1.03\ (.6547) + .0950\ (.93849) = 764$$

Calculation of the moment of inertial for a thin circular arc,

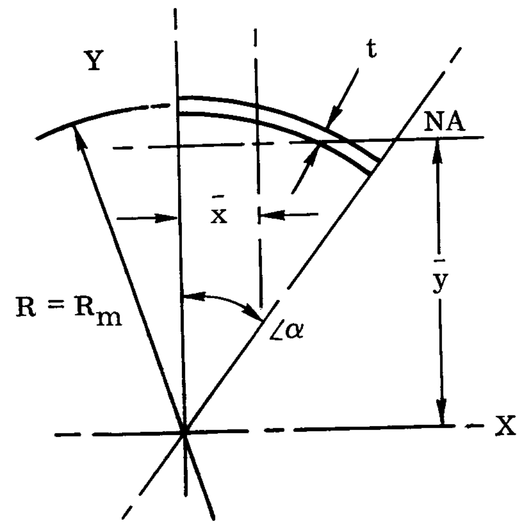

$$\bar{y} = R \sin\alpha/\alpha \qquad A = \alpha R t$$

$$I_{xo} = (R^3 t/2) \left[\alpha + (\sin 2\alpha/2\right]$$

$$I_{nax} = I_{xo} = (R^3 t/2)\ (2 \sin^2 \alpha/\alpha)$$

$$\bar{x} = (R/\alpha) \cdot (1 - \cos\alpha)$$

$$I_{yo} = (R^3 t/2) \left[\alpha - (\sin 2\alpha)/2\right]$$

$$\bar{y}^2 A = \left[(R \sin\alpha)/\alpha\right]^2 \alpha R t$$

$$\bar{y}^2 A = (R^3 t/2)\ (2 \sin^2 \alpha/\alpha)$$

$\alpha_1 = 64.05^\circ \quad t = .003$

$\alpha_2 = 69.80^\circ$

$R_2 = .56 \quad R_4 = .19$

$R_7 = .68 \quad R_9 = .35$

$w_3 = .33159 \quad W_8 = .0950$

$A = 2(3.0)\ (.003) = .018\ \text{in.}^2 = 6t$

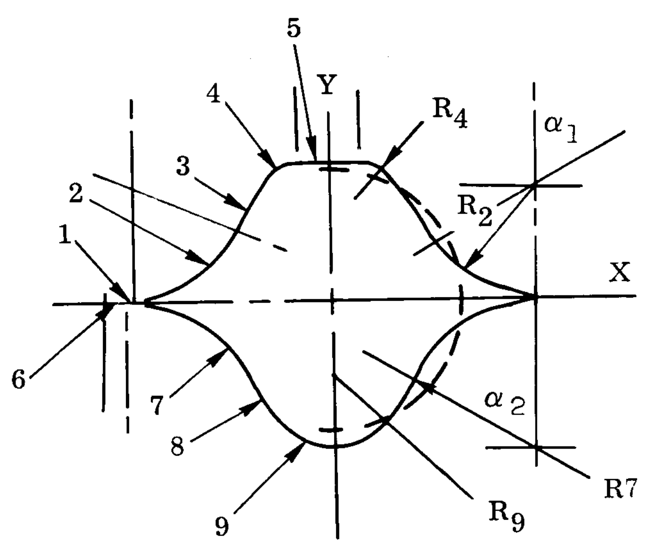

I_x tabulation:

	α	$\sin\alpha$	$\sin 2\alpha$	$\bar{y}$	d_I	I_{xo}	A_i	Σd^2	ΣAd^2	$\Sigma \frac{A}{t} d_{\bar{x}}$
2	64.05	.89918	.78694	.45044	.10956	.13271t	.62602t	-.19089	-.119503t	.068587
3					.46403	.00246t	.33159t	+.21532	+.071399t	.153868
4	64.05	.89918	.78694	.15283	.53000	.00518t	.21240t	+.28090	+.059663t	.145033
5					.72000		.15000t	+.51840	+.077760t	.108000
7	69.80	.93849	.64812	.52385	.15615	.24247t	.82840t	-.25004	-.207130t	-.129355
8					.48977	.00006t	.09500t		+.022788t	-.046528
9	69.80	.93849	.64812	.26963	.41400	.03306t	.42638t	+.17140	+.073080t	-.291486
						.41594t	3.0t		-.021943	.008119

$\sin 2\alpha_1 = \sin (2)(64.05) = \sin 128.1° = \sin 180 - 2\alpha_1 \sin 51.9°$

$\sin 2\alpha_2 = \sin 180 - 2 (69.8) = \sin 40.4°$

(2) $\bar{y} = R \sin\alpha/\alpha = .56 (.89918)/(64.05\pi/180) = .56 (.89918) 180/64.05\pi$

(4) $\bar{y} = .19 (.89918) 180/64.05\pi = .19 (.89918) (180)/201.21948$

(7) $\bar{y} = .68 (.93849) 180/69.8\pi = .68 (.93849) (180)/219.28368$

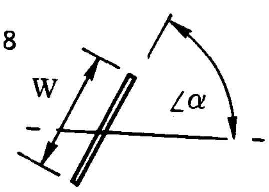

(8) $\bar{y} = .35 (.93849) 180/69.8\pi$

(2) $d = R_2 - \bar{y} = .56 - .45044$

(3) $d = R_2 (1 - \cos\alpha) + w_1 \sin\alpha/2 = .56 (1 - .43759) + .33159 (.89918)/2$

(4) $d = h - R_4 = .72 - .19 = .53$

(7) $d = R_7 - \bar{y}_7 = .68 - .52385 =$

(8) $d = R_7 (1 - \cos\alpha) + w_2 \sin\alpha/2 = .68 (1 - .34530) + .0950 (.93849)/2$

(9) $d = h - R_9 = .764 - .35$

(2) $I_{xo} = (R^3 t/2) \left[\alpha + (\sin 2\alpha)/2\right. = (.56^3 t/2 \quad 64.05\pi/180 + .78694/2\left.\right]$

$I_{xo} = (.56^3\ t/2) \left[1.11789 + .78694/2\right]$

(3) $I_{xo} = bh^3/12 \quad b = t/\sin\alpha \quad h = w \sin\alpha$

$I_{xo} = tw_3^3 \sin^2 \alpha/12 = t\ (.33159)^3\ (.88918)^2/12$

(4) $I_{xo} = (.19^3\ t/2) \left[1.11789 + .78694/2\right] = (.19^3\ t/2) \left[1.51136\right]$

(7) $I_{xo} = (.68^3\ t/2) \left[69.8\pi/180 + 64812/2\right] = .68^3\ t/2 \left[1.21824 + .32406\right]$

(8) $I_{xo} = tw_8^3 \sin^2 \alpha/12 = t\ (.095)^3\ (.93849)^2/12 = .00006$

(9) $I_{xo} = (.35^3\ t/2)\ (1.5423) = .03306t$

(2) $A = R_2\ \alpha_1\ t = .56\ (1.11789)\ t = .62602t$

(3) $A = w_3 t$

(4) $A = \alpha_1\ R_4 t = .19\ (1.11789)\ t$

(7) $A = .68\ (1.21824)\ t$

(8) $A = .35\ (1.21824)\ t$

(2) $\Sigma Ad^2 = A_2\ (d^2 - \bar{y}_2^2) = (.10956^2 - .45044^2)$

(7) $\Sigma Ad^2 = A_7\ (d_7^2 - \bar{y}_7^2) = (.15615 - .52385^2)$

(4) $d_{xo} = (d_{T4} + y_4') = (.53000 + .15283) = .68283$

(9) $d_{xo} = (d_T + \bar{y}) = (.41400 + .26963) =$

$h_T = h_1 + h_2 = .72 + .762 = 1.484$

$\bar{y}_{NA} = \Sigma Ad/\Sigma A = .008119t/3.0t = .002706$, very small

$I_{NA} = 2 \left[\Sigma I_{XO} + \Sigma Ad^2 - \bar{y}_{NA}^2 \quad (\Sigma A)\right]$

$= 2 \left[.41594t - 0\ .021943t = .002706^2\ (3t)\right]$

$I_{NA} = \dfrac{.788t}{}$ (does not include doublers, Reference page 32) Check case for 1.375 dia,

$I = \pi R^3 t = \pi\ (1.375/2)^3 t - (8.1669/8)\ t = 1.0209t$

$f_n = C\sqrt{gEI/wL^4}$, $E = 14.9\ (10^6)$, titanium at 350°

$w = .053778$ lb/in, Reference, p. 26, $I = (.95)\ (.788)\ t$, $L = 495$

$f_n = .560\sqrt{386.1\ (14.9)\ 10^6\ (.95)\ (.788)\ (.003)/.053778\ (495^4)}$

$f_n = \underline{\underline{.0358}}$ cps

For $f_n = .050 = \sqrt{I_{REQ}}\ K, f_{N1} = K\ \ I_1$

$I_{REQ}/I_1 = (f_N/f_{N1})^2 = (.050/.0358)^2 = (1.4)^2 = 1.96$

Tests on Beam (Prototype)

At ℄ support, h = .78

Full depth, h = 1.50

% full open = .78/1.50 = .52

% I at 52% open. Use 50% maximum, .75 average.

Tests of actual beam show, $(I_2 = .75I_1)$,

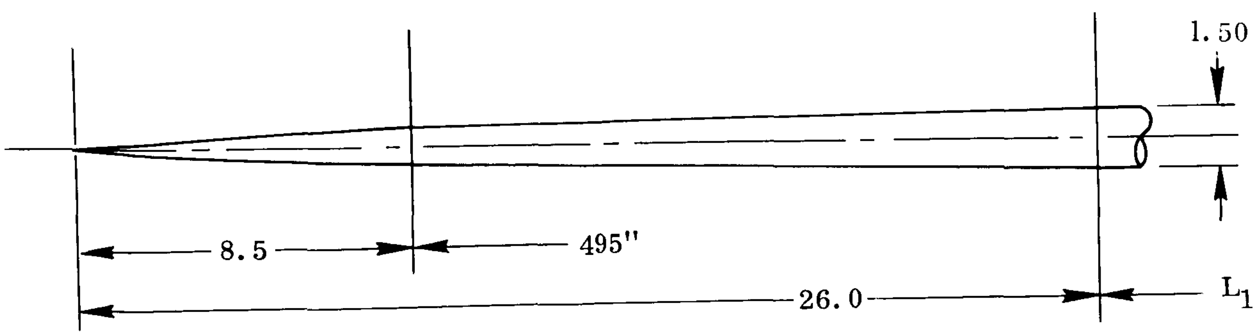

$L_1 = 495 - (26.0 - 8.5) = 477.5$

From p. 33, using new limits,

$\Delta_2 = (w/8E)\left[477.5^4/I_1 + (495^4 - 477.5^4)/.75I_1\right]$

$\Delta_2 = (w/8EI_1\left[519.8685\ (10^8) + (600.3725 - 519.8685)\ 10^8/75\right]$

$$\Delta_2 = 627.2071\ w10^8/8EI_1$$

$$\Delta_1/\Delta_2 = I_{RED}/I_1 = (600.3725)/627.2071$$

$$\Delta_1/\Delta_2 = I_{RED}/I_1 = .957$$

Adding doublers to basic section,

$$\Sigma Ad^2 = (.3)\ t\ (.72 + .003)^2 + 2\ (.2)\ t\ (.71)^2 = (.1568 + .2016)^t$$

$$I = I_o + \Sigma Ad^2 = (.788 + .1568 + .2016)\ t = 1.1464t$$

Assuming 100" of increase I and root reduction as per p. 33,

$$\Delta_2 = (w/8EI_o) \left\{ \left[x^4\right]_o^{395} + \left[N^4/(1.1464/.788)\right]_{395}^{477.5} + \left[x^4/.75\ (1.1464/.788\right]_{477.5}^{495} \right\}$$

$$\Delta_2 = (w/8EI_o) \left[395^4 + (.6874)\ (477.5^4 - 395^4) + .9165\ (495^4 - 477.5^4)\right]$$

$$\Delta_2 = (w10^8/8EI_o)\ (507.239)$$

$$\Delta_1/\Delta_2 = I_{EQ}/I_1 = (600.373/507.293) = 1.183$$

$$f_n = (1.1835)^{1/2}\ (.056)\ (.655) \quad \text{Ref: p. 31,}$$

$$(1.088)\ (.056)\ (.655) = .04\ \text{cps}$$

Use a doubler out to 125 inches to increase stiffness and raise frequency. Second, the reduction of the equivalent I, (moment of inertia), by 25% over the root length (8.5" to 26.0"), Reference p. 31, is on the conservative side. This is because the beam depth increases exponentially rather than straight line, and 50% reduction of moment at root (8.5") is probably also conservative.

Torsion and panel modes are considered to be higher than calculated for this cantilevered mode and this data, except for the preliminary analysis given on the next page, will not be presented until the final report.

Preliminary Analysis, Torsion Mode

For constant I_o,

$$\Delta = wL^4/8EI_o$$

For a reduced I at root section,

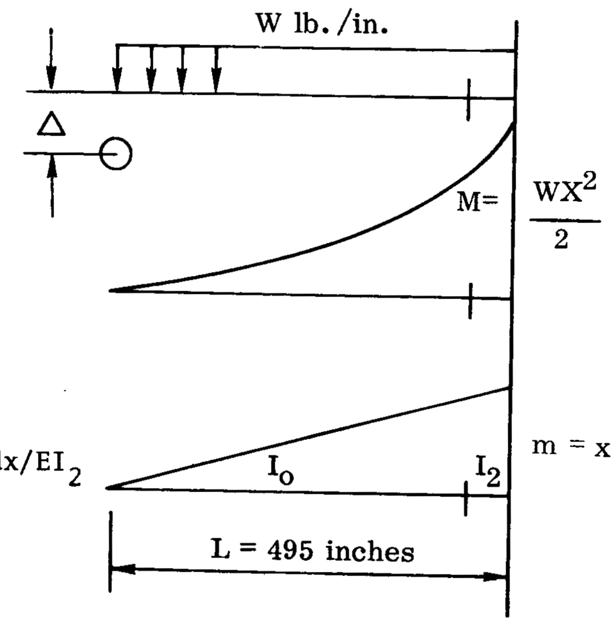

$$\ell = 13.oh - 8.75$$

$$= 13.0\ (1.69)\ -8.75 \quad 13.0$$

$$\Delta_2 = \int_o^{\ell} Mmdx/EI$$

$$\Delta_2 = \int_o^{482} Mmdx/EI_o + \int_{482}^{495} Mmdx/EI_2$$

$$\Delta_2 = \int_0^{482} wx^3dx/2EI_o + \int_{482}^{495} wx^3/2EI_2$$

$$\Delta_2 = (w/8E) \left\{ \left[x^4/I_o\right]_o^{482} + \left[x^4/I_2\right]_{482}^{495} \right\} = (w/8E)\left[482^4/I_1 + 60.628(10^8)/I_2\right]$$

Assuming a reductión in moment of inertia,

$$h_r = .80h_o, \text{ test data}$$

$$I_R = .80I_o \text{ (average)}$$

$$\Delta_2 = (w/8EI_o)\left[539.744\ (10^8) + 60.628\ (10^8)/.8\right]$$

$$\Delta_2 = (w10^8/8EI_o)\ (539.744 + 75.785)$$

$$\Delta_2 = 615.570\ w10^8/8EI_o$$

$$\Delta_1 = (w/8EI_o)\ (495)^4 = 600.373\ w10^8/8EI$$

$$\Delta_1/\Delta_2 = 600.373/615.570 = .975$$

Letting $\Delta_2 = wL^4/8EI_R = 495^4\ w/8EI_{RED} = 615.570\ w10^8/EI_o$

$$I_{RED} = .975\ I_o$$

$$f_n = c\ \sqrt{gEI/wL^4} = c\ \sqrt{8gEI/8wL^4} = 3.515\ \sqrt{386.1/8}\ /2\pi/\Delta_{ST}^{1/2}$$

$$f_n = 3.886/\Delta_{ST}^{1/2}$$

2.2.5 Solar Cell Installation

No additional studies or analysis were performed in this reporting period. All supporting analysis has been reported in References 1 and 2.

2.3 WEIGHT ANALYSIS

The calculated weight breakdown presented herein reflects the preliminary estimates of the effect of the design changes that were made during this reporting period. These consisted of the change in the position of the wrap drum axis with respect to the mounting arrangement at the ends and, the revised mechanism concept for driving the beams and controlling tension in the wrapped substrate.

For comparison, where weight estimates have changed, the weight values as reported in the second quarterly report are noted in "brackets". The original estimated weights that were established for design control purposes are listed under "Target Weights".

Calculated weights are based on nominal sheet thicknesses and drawing tolerances.

The power to weight capabilities of the solar array are calculated considering various solar cell power output levels, combined with nominal and maximum expected solar array weights. These values establish a reasonable envelope of obtainable performance and indicate that the objective of the contract can be achieved. The equation used for these calculations is:

$$\text{watts/pound} = \frac{(\text{Cell Output})\ (\text{Gross Cell Area})}{(\text{Nominal Array Wt.})\ (\text{K})}$$

Cell output values remain as reported in the second quarterly report.

TABLE 5

DRUM SUPPORT AND GUIDE SLEEVE MOUNT ASSEMBLY

Item		Cal. Wt. Machined Structure Concept	Target Weight
1. Support Channels	Items 1,2,3	-- (.375)	0.456
2. Slide Guide Fitting		0.857 (.808)	--
3. Slide Guide		--	0.200
4. Slide		0.102	0.171
5. Slide Retaining Angles		0.052	--
6. Bulkhead and Adjustment Screws		--	0.108
7. Springs		0.140	0.140
8. Spring Fittings		0.014	0.027
9. Mount Lugs			0.074
10. Shims			
11. Mount Bolts		0.046	
12. Helicoil Inserts		0.024	
13. Retaining Screws		0.026	
14. Stop Mechanism		0.303	
TOTAL WEIGHT		1.564 (1.891)	1.176

TABLE 6

BEAM GUIDE SLEEVES

Item	Cal. Wt.		Target Wt.
1. Side Plates O/B	0.2513	(.3203)	0.3130
2. Side Plate I/B	0.1613	(.2014)	
3. Top Plates	0.1006	(.1764)	0.2660
4. Bottom Plates	0.0824	(.0559)	
5. End Plates I/B	0.0364	(.1457)	0.0540
6. End Plate O/B	0.0270	(.0148)	
7. Internal Bulkheads	0.0311	(.1184)	0.1310
8. Attach Angles	0.0601	(.0380)	
9. Frame Angle	0.0843	(.0843)	
10. Closing Angle		(.0096)	
11. Guide Inserts	0.0842		
12. Top Plate (Support)	0.0432		0.4290
13. Support (Guide Insert)	0.2284		
14. Angles (Clutch End)		(.0075)	
TOTAL	1.1903	(1.4847)	1.1930

TABLE 7

WRAP DRUM ASSEMBLY

Item	Cal. Wt. Slip Ring Concept	Target Wt.
1. Skin (Mag.)	4.794	5.696
2. Intermediate Rings	0.111	0.115
3. Harness Retaining Ring		0.106
4. End Plate Rings		0.113
5. End Plates	2.746	1.786
6. Harness Spool		0.101
7. Roller Brgs	0.160	
8. Electrical Harness		1.600
9. Electrical Wiring	0.600	
10. Bushing Supports		0.167
11. Spindle and Bolt Attachment	0.260	
12. Snap Rings	0.009	
13. Sleeve Holder	0.076	
14. End Caps	0.065	
15. Sleeves	0.246	
16. Sleeve Flanges	0.056	
17. Contact Rings	0.098	
18. Ring Holders	0.164	
19. Insulator	0.005	
20. Contacts		
21. Screws	0.010	
TOTAL	9.400	9.684

TABLE 8

SPACECRAFT MOUNT ASSEMBLY

Item			Cal. Wt. Alumin. Support Structure Concept		Target Wt.
1.	Top and Bottom Plates	(.025)	0.8992	(1.0470)	0.466
2.	Side Plates	(.025)	0.7322	(.6966)	0.368
3.	Internal Bulkheads	(.025)	0.3680	(.3498)	0.074
4.	Closure Angles		0.2331	(.2596)	0.093
5.	Spacecraft Mount Fttg's	(1)	0.0825	(.0669)	0.033
6.	Drum Mount Fttg's	(4)	0.3889	(0.374)	0.039
7.	Center Attach Fttg's	(2)	0.2734	(.0366)	0.098
8.	Truss Tubes	(4)	0.5330		1.787
9.	Center Truss Tubes	(2)		(.0827)	0.029
10.	Truss Pins	(12)	0.1176		0.132
11.	Fasteners Attach Fttg's (#6 alum. huckbolts)	(24)	0.0960		
12.	Corner Bracket	(2)		(.0406)	
	TOTAL WEIGHT		3.7239	(3.0799)	3.119

TABLE 9

PANEL ASSEMBLY

Item	Cal. Wt. Kapton Substrate Concept	Target Wt.
1. Substrate (0.001 Kapton)	2.016	3.233
2. Substrate (0.001 Fiberglass)		
3. Substrate-Beam Attach Medium (Silicone Impregnated 0.004 Fiberglass)	0.089	0.050
4. Substrate Intersheet Attach Medium (Silicon Impregnated 0.004 Fiberglass)	0.047	0.045
5. Side Beams (Basic)	3.029	3.272
6. Tip Intercostal	0.263	
7. Stop Damper Pad	0.012	0.502
8. Substrate Doublers (240)	0.061	0.082
9. Drive Strips (1/2" Wire)	0.536	0.599
10. Damper Pads	1.914	2.527
11. Adhesive (Item 10)	0.764	
12. Outer Wrap Blanket		0.158
TOTAL WEIGHT	8.731	10.469

TABLE 10

DEPLOYMENT/RETRACTION SYSTEM

	Item	Cal. Wt. Redundant System Concept		Target Wt.
	Extension System			
1.	Drive Motor and Pinion	2.000		0.756
2.	Motor Brace	0.021		0.017
3.	Motor Mount	0.017		0.023
4.	Idlers	--	(.240)	0.240
5.	Torque Tube Shaft	0.234		0.090
6.	Drive Sprockets	0.208		0.230
7.	Torque Tube End Caps	0.106		0.111
8.	Torque Tube	1.481		1.607
9.	Torque Tube Support	0.234		
10.	Bushings and Retainers	0.033		0.071
11.	Roll Pins	0.013		
12.	Attach Bolts (Shaft)	0.060		
13.	Attach Bolts (Motor)	0.040		
14.	Limit Switch and Drive	0.200		0.100
15.	Electrical Wiring	0.200		
	SUBTOTAL	4.847		
	Retraction System			
16.	Retraction Drive Motor	1.000		
17.	Drive Shaft-Pulley		(.107)	
18.	Drum Pulley and Clutch		(.206)	
19.	Spring Belt		(.150)	
20.	Belt Retainer		(.021)	
21.	Fasteners	0.035		
	SUBTOTAL	1.035		
	TOTAL WEIGHT	5.882	(5.606)	3.245

TABLE 11

WEIGHT SUMMARY

Array Subassembly Item	Cal. Wt. Selected Configuration		Target Wt.
Drum Support and Guide Sleeve Mount Assembly	1.564	(1.891)	1.176
Beam Guide Sleeves	1.190	(1.485)	1.193
Wrap Drum Assembly	9.400		9.684
Spacecraft Mount Assembly	3.724	(3.080)	3.119
Panel Assembly	8.731		10.469
Deployment/Retraction System	5.882	(5.606)	3.245
TOTAL STRUCTURAL WT.	30.492	(30.193)	28.886
Solar Cell and Electrical Installation Wt. (2 x 2 x 0.008 with 0.003 CG. - 250.7 ft^2 @ 0.178 lb/ft^2)	44.627		47.636
TOTAL ARRAY WT.	75.119	(74.820)	76.522

Power/Weight Summary

The watts/pound capability of the solar array configuration, as influenced by the various considerations discussed in this section, is determined as follows:

a. Nominal solar array weight with 10.0 watts per square foot solar cell power output.

$$\text{Watts/Pound} = \frac{(10)\ (250.72)}{75.119} = \underline{33.38}$$

b. Maximum solar array weight which allows for a 5% growth of the array during detail design and a 4% tolerance for material and fabrication tolerances with power at 10 watts/square ft.

$$\text{Watts/Pound} = \frac{(10)\ (250.72)}{(75.119)\ (1.04)\ (1.05)} = \underline{30.57}$$

Ryan Selected Configuration:

c. Solar Array with

1) Nominal weight - 75.119 pounds

2) 2 x 6 - 0.008 cells, 0.003 coverglass with power output of 10.3 watts/ft^2 which is more consistent with the design,

$$\text{Watts/Pound} = \frac{(10.3)\ (250.72)}{75.119} = \underline{\underline{34.38}}$$

d. Maximum solar array weight as defined in c.2 above with power output of 10.3 watts/ft^2.

$$\text{Watts/Pound} = \frac{(10.3)\ (250.72)}{(75.119)\ (1.04)\ (1.05)} = \underline{\underline{31.48}}$$

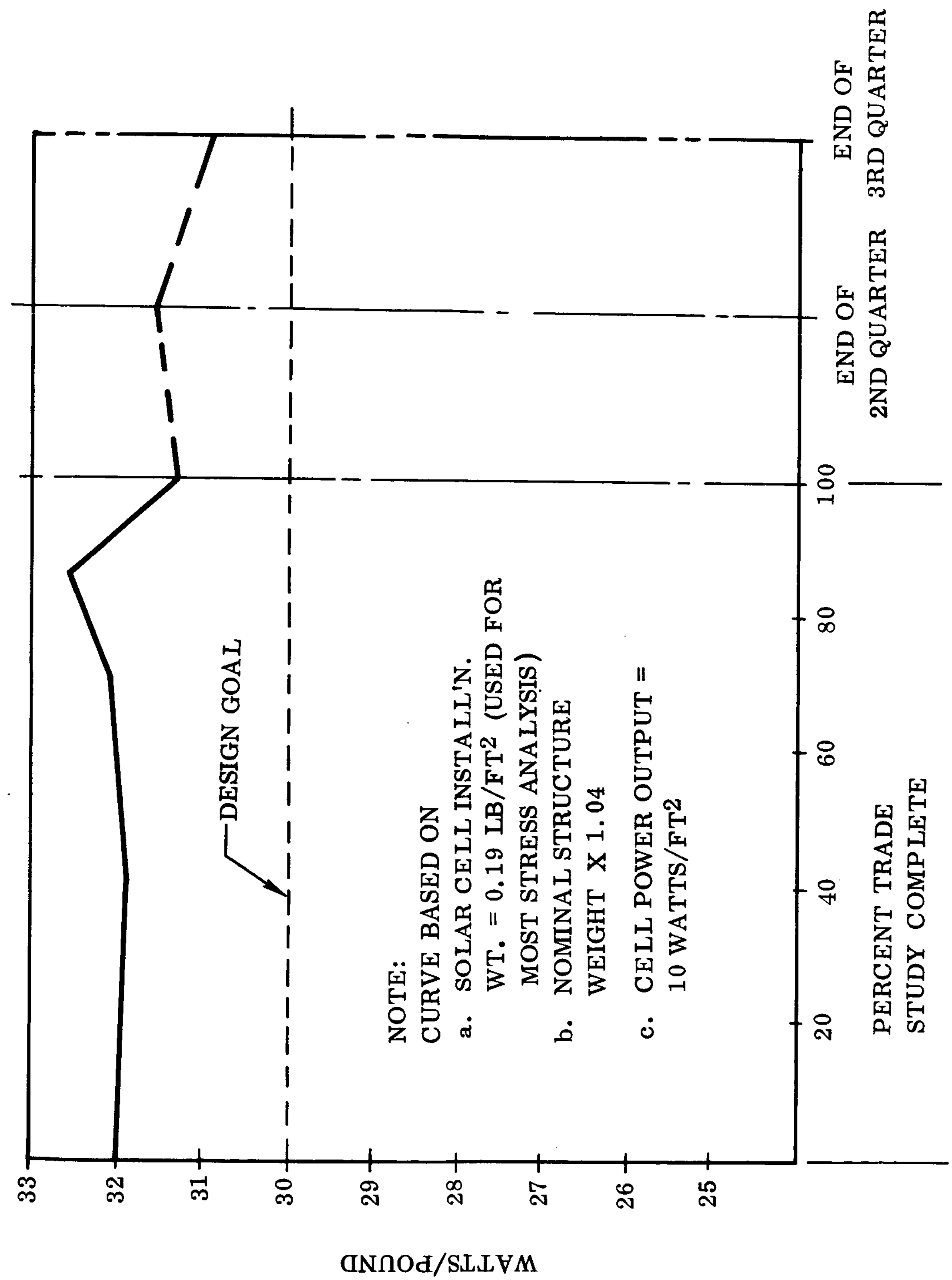

Figure 5 Power/Weight Monitor

Figure 5 Power/Weight Monitor

2.4 TESTING-STOWED PANEL VIBRATION

A test was conducted to determine the effects of various levels of sinusoidally induced vibration, up to 4g (0 - pk), on (1) stowed panel wrap mode shapes, (2) degree of damping provided by varying number of panel wraps, (3) linearity of natural frequencies, (4) wired solar cell modules, and (5) transmissibilities through wrap drum bearings and end plates. A full size 12-inch diameter x 86-inch long wrap drum was mounted in each end to rigid aluminum end fixtures. Figure 6 shows the test assembly and fixtures. One-half of the total number of wraps were used for reasons of reduced costs. The total mass was actually simulated using 1 ft^2 of solar cells, each wrap, and 2 cm x 2 cm magnesium chips (representing 0.178 lbs/ft^2 of solar cell installation). The balance of the mass was represented by use of copper chips which were bonded to two wraps of the 1 mil Kapton substrate. Results of the test will be summarized and presented in the final report.

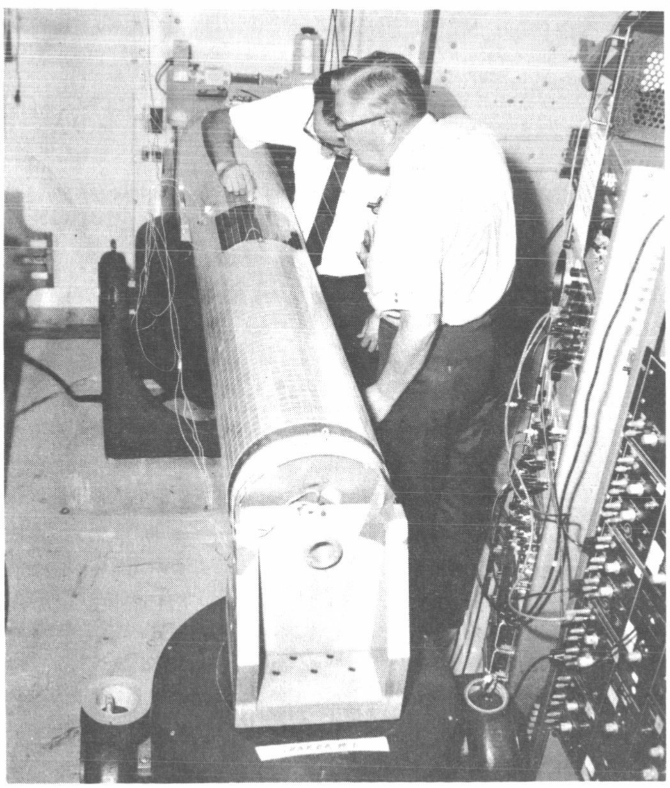

Figure 6 Stowed Panel Vibration Test Setup

3.0 FABRICATION-DEMONSTRATION MODEL

Fabrication of a full scale demonstration model of the solar array began in this reporting period. The deployed substrate area will be approximately 251 square feet, fabricated as 13 substrate modules. Width and length will be equivalent to the detailed engineering design that has been performed.

The substrate modules are being fabricated from the specified material, one-mil Kapton. A facsmile solar cell installation will be used. Substrate-to-beam attachment and the module-to-module joint arrangement will be representative of the design of the type approval array. A typical pattern of interwrap damper pads will be bonded to the Kapton substrate.

The wrap drum shown in Figure 7 was fabricated earlier to support vibration tests and will now be used in the demonstration model. Wrap drum support structures, simulating the revised support concept discussed in Section 2.1.1, are in work.

One of the two deployable beams has been formed and assembled; the second is in process of construction. Figures 8 and 9 show a forty-five foot long beam of 0.003 inch 6 AL-4V titanium alloy, fully rolled up and partially unrolled. Figure 10 shows the corrugated rack on which a pinion will engage and drive the beam on or off the wrap drum. The splicing technique used in the manufacture of the beams can be seen in Figures 10 and 11.

No manufacturing problems have been encountered that have not been resolved.

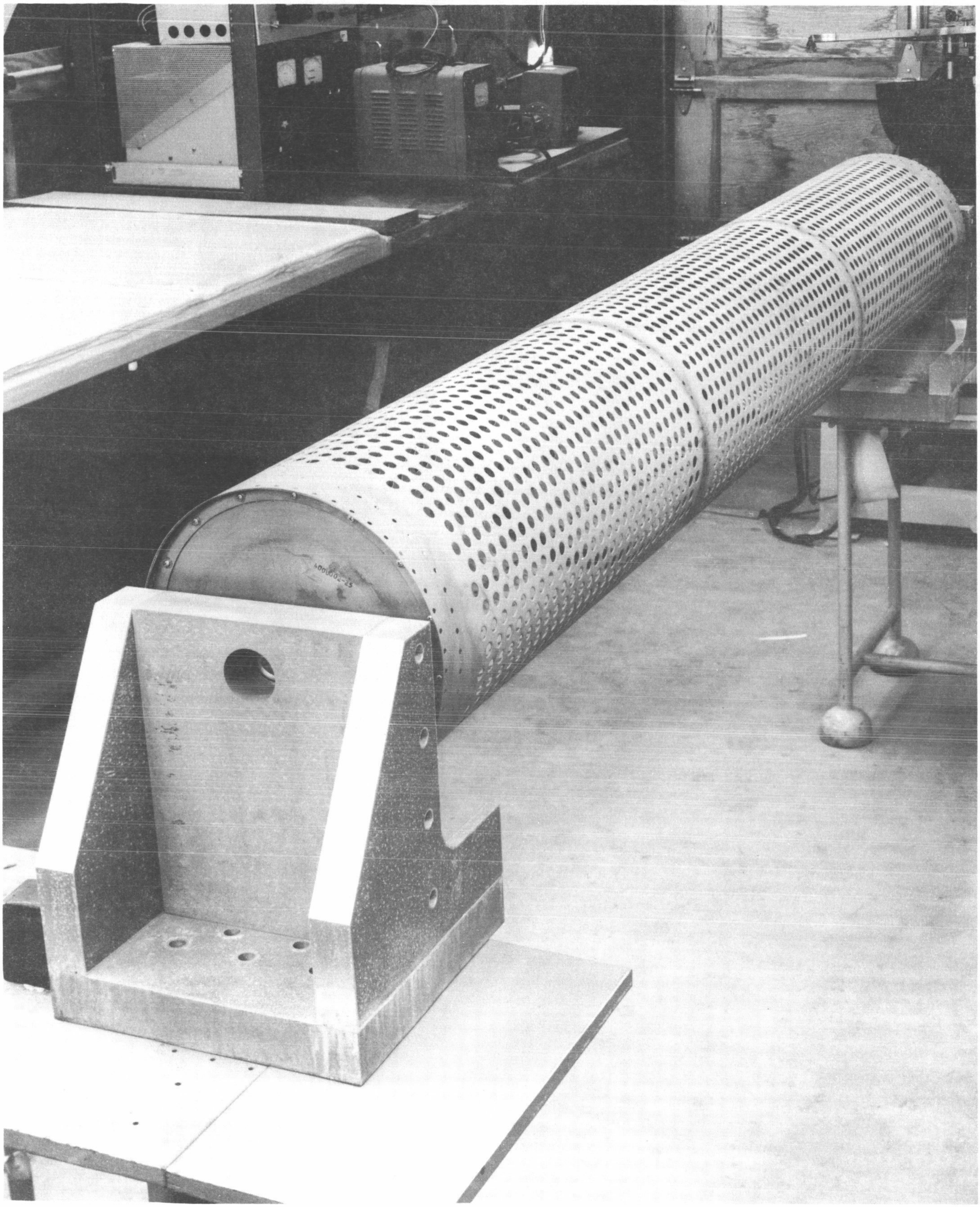

Figure 7 Wrap Drum Assembly

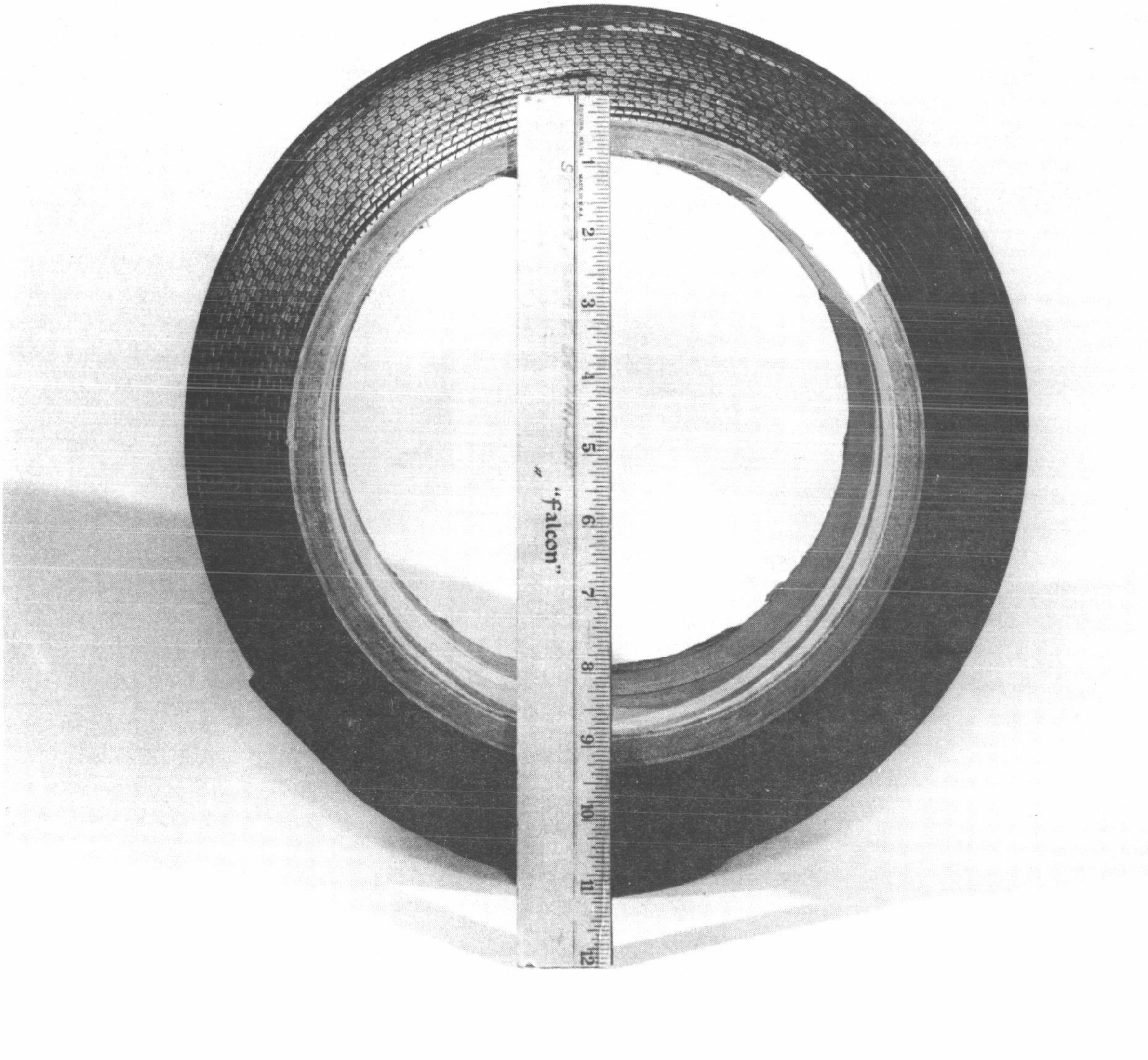

Figure 8 Deployable Beam-Forty-Five Length, Rolled

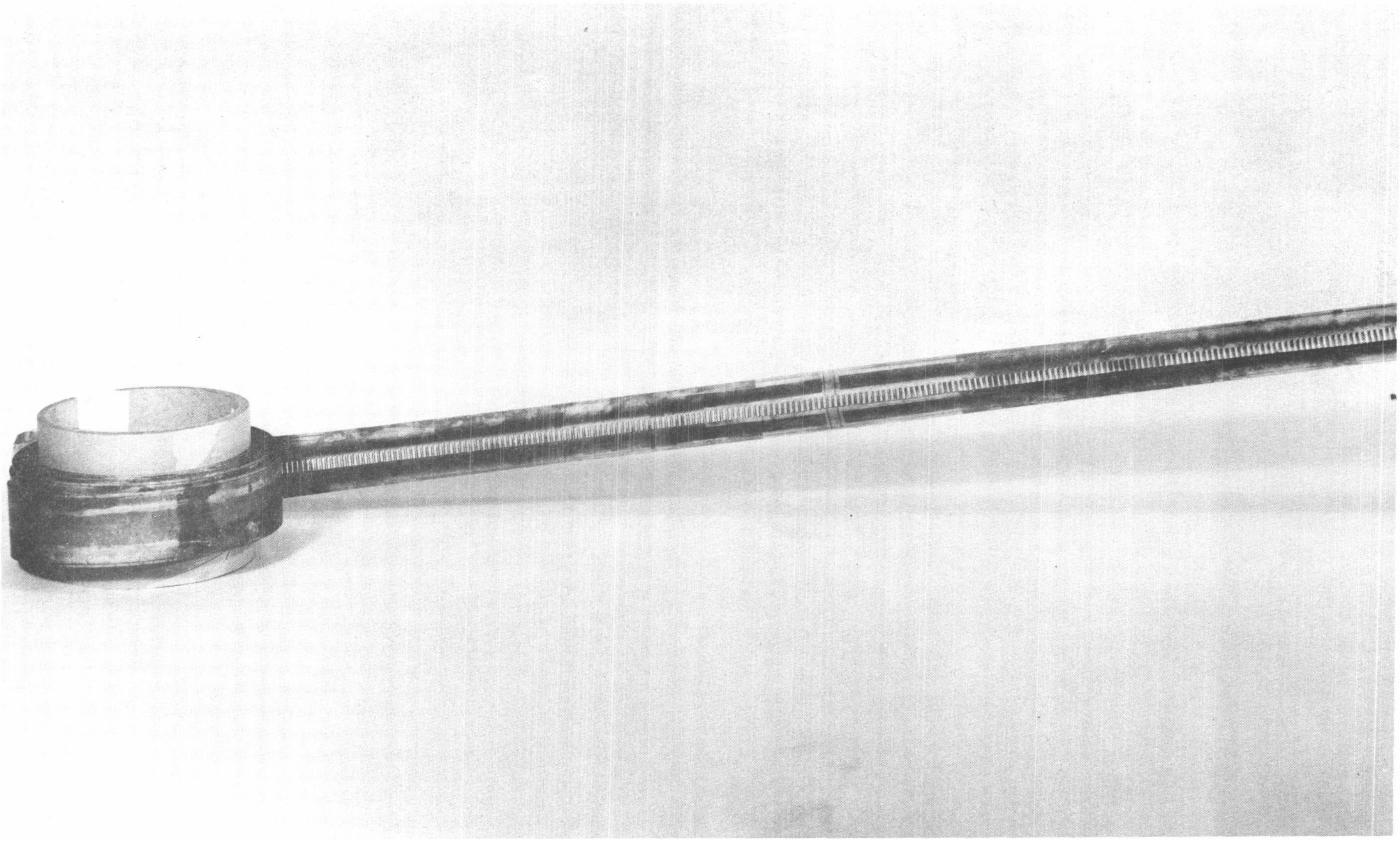

Figure 9 Deployable Beam - Partially Unrolled

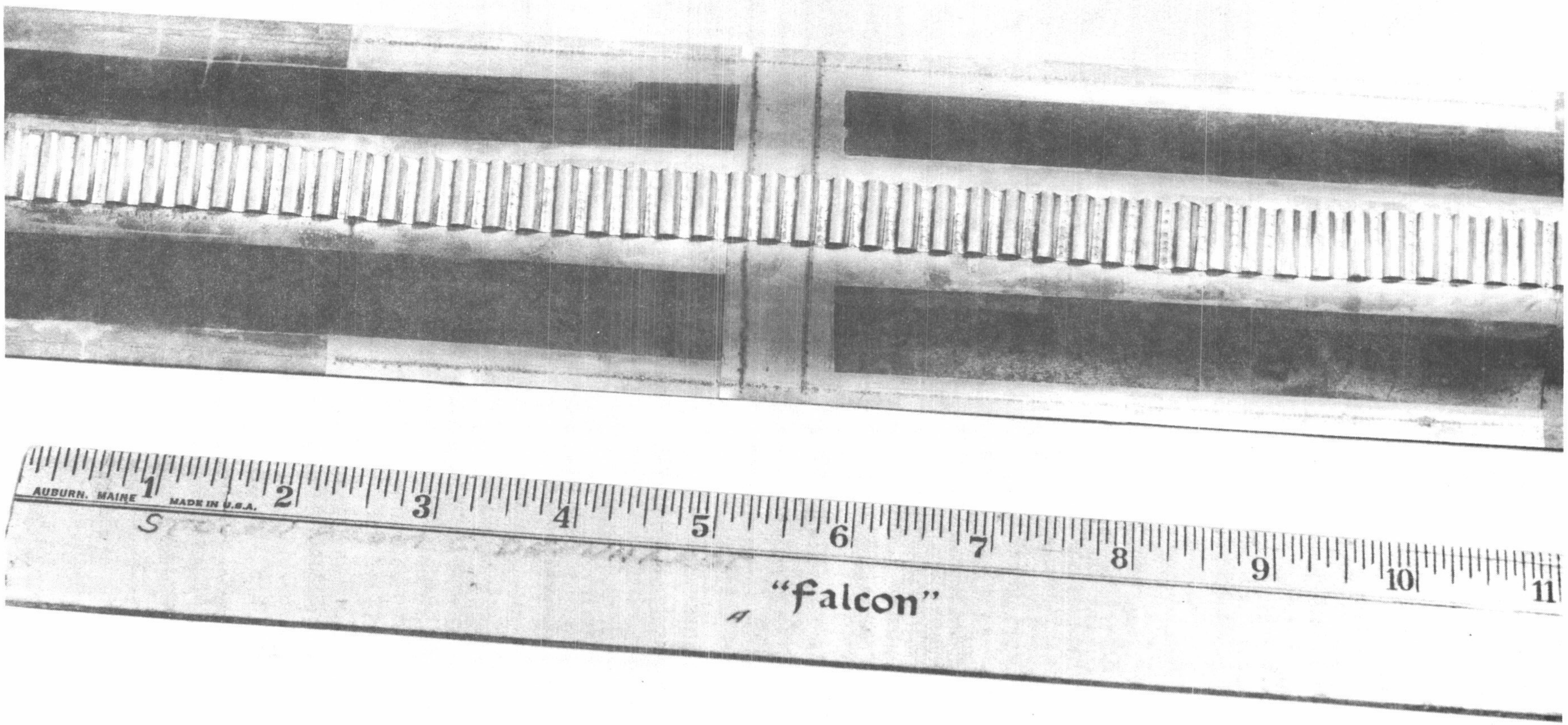

Figure 10 Deployable Beam With Corrugated Rack Installation

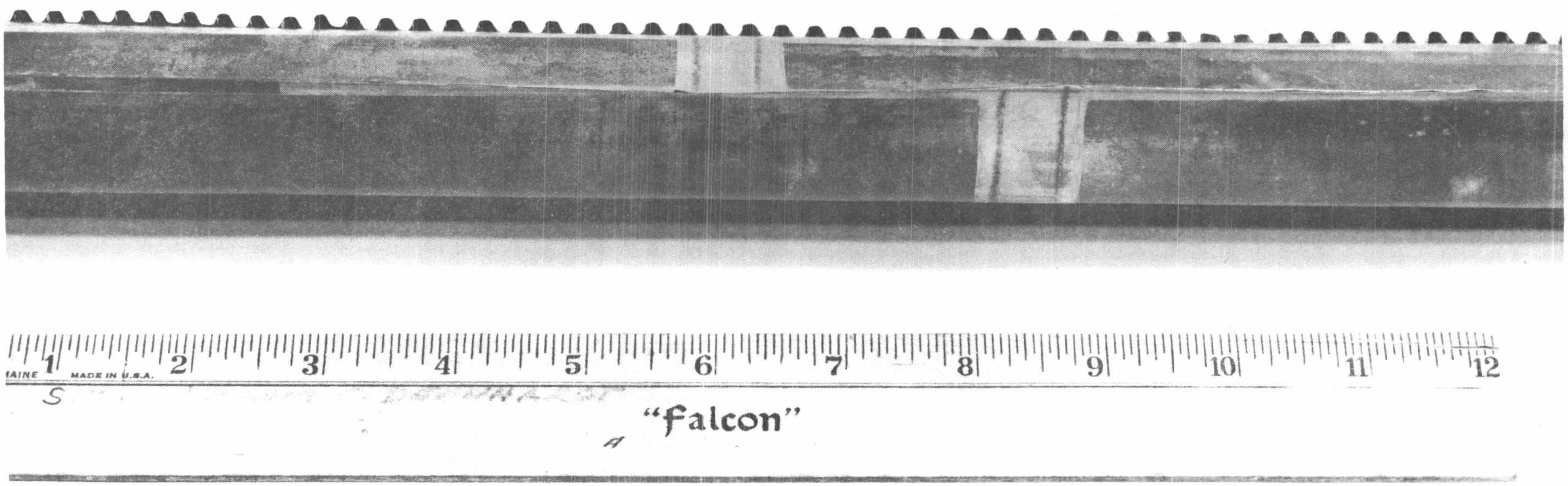

Figure No. 11 Deployable Beam Showing Beam Splice Design

4.0 CONCLUSIONS

Construction of the quarter scale model demonstrated that improvements were needed in the support structure and slide action of the drum spindle, also in the drive system as it influences tension in the wrapped substrate. A modification to the design is necessary (as discussed in Section 2.1.1) to overcome these deficiencies.

With incorporation of those improvements that have been noted, it is felt that engineering designs and analyses substantiate the Ryan concept as being well suited to the objectives of the program. There is good confidence that the 30-watt/pound, power-to-weight ratio can be achieved with this concept.

5.0 RECOMMENDATIONS

No recommendations are made other than continuation of the work planned to achieve the design and performance objectives of this contract. The scope of work and Ryan's method of approach are set forth in this Contractor's program plan and in the interim work accomplishment reports that have been submitted. It is the Company's intent to proceed with the manufacture of the demonstration model and the incorporation of the design improvements, as discussed in this report, in the model and in the detail design and supporting analyses.

6.0 NEW TECHNOLOGY

The new technology disclosure, reported in the Second Quarterly Report, Reference 2, concerning Application of Ultra Thin (1.3-mil) Coverglass on Silicon Solar Cells, was formally submitted 5 March 1968. It was previously reported as submitted 19 January 1968.

No other items of a "New Technology" nature have been identified.

7.0 REFERENCES

1. First Quarterly Report on the Feasibility Study, 30 Watts Per Pound, Rollup Solar Array, Report 40067-1, Ryan Aeronautical Company, 10 November 1967

2. Second Quarterly Report on the Feasibility Study, 30 Watts Per Pound, Rollup Solar Array, Report 40067-2, Ryan Aeronautical Company, 15 January 1968

3. S. P. Timoshenko and S. Woinowsky-Krieger, Theory of Plates and Shells, Second Edition, Mc Graw-Hill Book Co., New York, 1959

4. R. J. Roark, Formulas for Stress and Strain, Mc Graw-Hill Book Co., New York, 1954

5. Connecticut Hard Rubber Co. Bulletin for Cohrlastic Coated Fabrics